INFORMATION TO USERS

This manuscript has been reproduced from the microfilm master. UMI films the text directly from the original or copy submitted. Thus, some thesis and dissertation copies are in typewriter face, while others may be from any type of computer printer.

The quality of this reproduction is dependent upon the quality of the copy submitted. Broken or indistinct print, colored or poor quality illustrations and photographs, print bleedthrough, substandard margins, and improper alignment can adversely affect reproduction.

In the unlikely event that the author did not send UMI a complete manuscript and there are missing pages, these will be noted. Also, if unauthorized copyright material had to be removed, a note will indicate the deletion.

Oversize materials (e.g., maps, drawings, charts) are reproduced by sectioning the original, beginning at the upper left-hand corner and continuing from left to right in equal sections with small overlaps.

Photographs included in the original manuscript have been reproduced xerographically in this copy. Higher quality 6" x 9" black and white photographic prints are available for any photographs or illustrations appearing in this copy for an additional charge. Contact UMI directly to order.

ProQuest Information and Learning
300 North Zeeb Road, Ann Arbor, MI 48106-1346 USA
800-521-0600

UMI®

DISSERTATION

DISSOLUTION OF ORGANIC LIQUIDS IN GROUNDWATER

Submitted by

Sunisa Smittakorn

Department of Civil Engineering

In partial fulfillment of the requirements

for the Degree of Doctor of Philosophy

Colorado State University

Fort Collins, Colorado

Summer 2001

ProQuest Information and Learning Company
300 North Zeeb Road
P.O. Box 1346
Ann Arbor, MI 48106-1346

COLORADO STATE UNIVERSITY

April 26, 2001

WE HEREBY RECOMMEND THAT THE DISSERTATION PREPARED UNDER OUR SUPERVISION BY SUNISA SMITTAKORN ENTITLED DISSOLUTION OF ORGANIC LIQUIDS IN GROUNDWATER BE ACCEPTED AS FULFILLING IN PARTIAL REQUIREMENTS FOR THE DEGREE OF DOCTOR OF PHILOSOPHY.

Committee on Graduate Work

Committee Member

Committee Member

Committee Member

Adviser

Department Head

ABSTRACT OF DISSERTATION

DISSOLUTION OF ORGANIC LIQUIDS IN GROUNDWATER

Among the most pervasive and persistent sources of groundwater contamination are organic liquids that enter the subsurface from leaks, spills, and improper disposal. Organic liquids with specific gravity greater than unity are known as DNAPLs (dense non-aqueous phase liquids) and these are especially troublesome because they tend to sink well below the watertable.

Remediation technologies for subsurface source zones containing DNAPL are not yet able to achieve levels of mass removal sufficient to restore the groundwater or to meet regulatory requirements. Therefore, it is natural to inquire about the benefit of partial mass removal. This subject has been and is being addressed by many researchers for single-component DNAPLs. This dissertation considers the dissolution of multi-component DNAPLs; a process that is inherently unsteady.

A mathematical technique called TMASST (transient multiple analytical source superposition technique) was developed to calculate the unsteady rate of dissolution of both single and multiple component DNAPLs. Source zones are thought to be comprised of many subzones that contain DNAPL. The number, location, and geometry of the subzones are not known. This problem is circumvented by synthesizing a new mass transfer rate coefficient that applies to the source zone as a whole. This field-scale parameter is much smaller in magnitude than the values of mass transfer rate coefficient measured in laboratory experiments.

Calculations show that multi-component DNAPLs dissolve more slowly than single-component DNAPLs. Individual component solubilities and the type of mixture are the important DNAPL characteristics affecting the source longevity. Sources are estimated to persist for many decades and the dissolved concentrations of DNAPL components in waters passing through the source zone are calculated to remain well above the regulatory limits until virtually all the DNAPL has been dissolved away.

Sunisa Smittakorn
Civil Engineering Department
Colorado State University
Fort Collins, CO 80523
Summer 2001

ACKNOWLEDGEMENTS

I would like to express my gratitude and appreciation to my adviser, Professor David McWhorter, for his support, encouragement, guidance and patience throughout this research. I also express my gratitude and appreciation to my co-adviser, Professor Deanna Durnford for her support, encouragement and guidance. I express my sincere thanks to my committee members Professor Charles Shackelford and Professor David Zachmann for their advice, guidance.

I would like to thank Dr.Tom Sale for his help, support and encouragement. I also thank Professor Art Corey, Mrs. Vera Corey, Professor Paul Heyliger, Dr. Stela Cota, Professor Susanne Foitzik, Tobias Wittig and friends from Thammasat university for their support and encouragement. I gratefully acknowledge the scholarship from the Thai government throughout my study.

I deeply appreciate the support and encouragement from my parents, sisters and brother back in Thailand. Lastly, the support and encouragement from my my husband, Watanachai and my daughter, Muchima is also deeply appreciated.

DEDICATION

To my parents, Jutharat and Paiboon Katchamart.

CONTENTS

LIST OF TABLES

LIST OF FIGURES

CHAPTER 1

Introduction

Dense nonaqueous phase liquids (DNAPL) are organic liquids with specific gravities greater than water. DNAPL contamination of groundwater originates from various operations [1]

- wood treatment operations (cresote)
- manufactured gas plants (coal tar)
- transformer oil production, reprocessing and disposal facilities (PCBs and chlorinated solvents)
- chemical industry facilities (chlorinated solvents, pesticides, herbicides, and other dense organic compounds)
- steel industry coking operations (coal tar)
- dry cleaners (chlorinated solvents)
- electronic instrument manufacturers (chlorinated solvents)
- machine shops (chlorinated solvents)
- metal works (chlorinated solvents)
- waste disposal facilities (all types)

By the 1980 public law, 1.6 billion dollars was provided through the year 1985 for cleaning up contaminated sites. The Superfund law was signed on Oct 17, 1986. This law provided tougher standards and a tighter schedule. Since then, there have been several attempts to find methods to remediate groundwater contaminated by DNAPLs. Such methods rely on physical, biological and chemical processes. Some of them are: the pump and treat system, soil vacuum extraction (SVE), biodegradation, steam stripping and soil flushing. For a while, the pump and treat system was considered to be a way to remove NAPLs out of the groundwater system. However, Hunt *et al.* [14] concluded that because of rate-limited mass transfer in the dissolution process, groundwater extraction is not an efficient way to remove NAPLs within a reasonable time. There still is no strong evidence that conclusively shows a successful source zone remediation with sound engineering and economic aspects. The US. EPA workshop summary on dense nonaqueous phase liquids in 1992 [1] concluded that there are no proven technologies that will reduce the mass of subsurface DNAPL to the required levels for full restoration of a contaminated aquifer.

A project summary of evaluation of technologies for in-situ cleanup of DNAPL contaminated sites by US. EPA. in 1994 [12] concluded that even though there are some technologies that show promise for cleaning up source zone NAPL (e.g. the thermal processes) these techniques may not be able to succeed to the levels which are required by the law. Use of these technologies, along with long term plume management, was recommended in that report. Freeze and McWhorter [10] pointed out that with today's technologies, the mass-removal efficiency rate has been quite low. In other words, only partial restoration has been achieved. They also supported Cherry *et al.* [5] that the primary goal of remediation should be short-term risk reduction, and that future research is needed in order to improve the mass-removal

processes. These ideas motivate the attempts to gain knowledge about the benefits of partial removal of mass.

In order to be able to manage contaminated groundwater sites successfully, it is also important to understand the DNAPL dissolution process. This research is an attempt to learn more about the dissolution process of multicomponent DNAPLs. There are 5 chapters in this research.

- Chapter 2; Dissolution of DNAPLs. The general background of the dissolution of DNAPLs are presented including the earlier works in this area.
- Chapter 3; The transient state dissolution of DNAPLs. A semi-analytical solution is used to develop a mathematical model to examine the dissolution of the single and multicomponent DNAPLs in the transient state.
- Chapter 4; The field-scale mass transfer rate coefficient. The field-scale mass transfer rate coefficients are estimated.
- Chapter 5; Case studies. Several case studies are examined.
- Chapter 6; Conclusions. The results of the findings in the case studies are presented.

CHAPTER 2

Dissolution of DNAPLs

2.1 Conceptual model of the DNAPL source zone

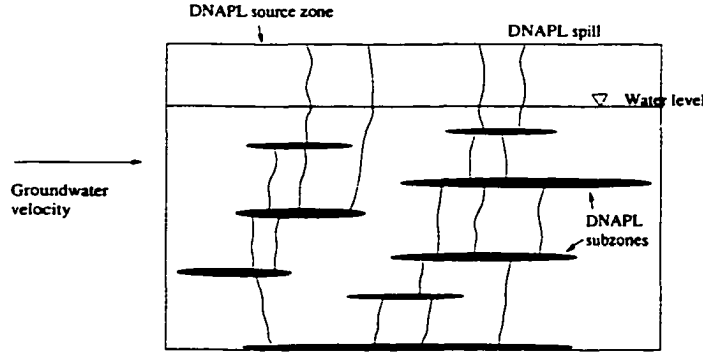

Figure 2.1: Conceptual model of DNAPLs present in groundwater

When a dense non-aqueous phase liquid (DNAPL) is released onto the ground, it makes its way downward due to gravitational and capillary forces. Once it reaches the water table, because its specific gravity is greater than unity, DNAPL tends to sink to the bottom of the aquifer. If there is a finer layer of porous media on its course, the DNAPL pressure must exceed the water pressure by a threshold amount (the entry pressure) in order to pass through (Corey [8]). This entry pressure is dependent on the interfacial tension between the DNAPL and the water and the size of the pore throats. In fact, it is inversely proportional to the size of the pore throats. As a result, a high DNAPL pressure is required for DNAPL to pass through the finer layers, [22]. Until the entry pressure is overcome, the pool of DNAPL is formed. The pool may

then break loose into vertical fingers and travel downward. And if there exists another finer porous medium, then another DNAPL pool will develop. Figure (2.1) shows the conceptual model of pools and fingers based on laboratory works by Schwille [28] and Kueper *et al.* [17]. In this figure, one pool of DNAPL will be defined as a subzone. In the groundwater system, several subzones connected by vertical fingers, is referred as the DNAPL source zone.

2.2 The mass transfer rate

In a system where the NAPL and the aqueous phase coexist, a chemical imbalance exists. This imbalance causes the transfer of mass from the higher concentration in the DNAPL to the lower concentration in the aqueous phase. There are many mathematical models that have been advanced to characterise this mass transfer process. One of them is called the linear-driving-force model or the stagnant film model [29] used by many researchers (e.g. Hunt *et al.* [14], Miller *et al.* [20] and Powers *et al.* [25])). The assumption in this model is that there is a linear relationship between the mass transfer rate and the difference between the equilibrium concentration at the NAPL-water interface and the bulk aqueous phase concentration:

$$\dot{M} = k_l a(C_s - C_a) \tag{2.1}$$

where $\dot{M}$ is the mass transfer rate from the NAPL phase to the aqueous phase per unit bulk volume of porous medium ($\mathrm{M{\cdot}L^{-3}{\cdot}T^{-1}}$), k_l is the mass transfer coefficient ($\mathrm{L{\cdot}T^{-1}}$), a is the specific interfacial area between the NAPL phase and the aqueous phase ($\mathrm{L^{-1}}$), C_s is the equilibrium concentration or the solubility limit at the NAPL-water interface and C_a is the concentration in the bulk aqueous phase ($\mathrm{M{\cdot}L^{-3}}$).

2.3 The mass transfer rate coefficient

A practical problem using the mass transfer coefficient to obtain the mass transfer rate occurs because it is quite difficult to determine the specific interfacial area between the NAPL phase and the aqueous phase. Miller *et al.* [20] discussed the problems concerning the measurement of the specific interfacial area between the NAPL phase and the aqueous phase. To avoid this problem, another empirical parameter called the mass transfer rate coefficient is introduced. The mass transfer rate coefficient is a parameter that lumps the specific interfacial area and the mass transfer coefficient together. The relationship between k_l and K_L is (after Miller *et al.* [20]).

$$\frac{1}{V}\frac{dm}{dt} = ak_l(C_s - C_a) = K_L(C_s - C_a) \tag{2.2}$$

where V is the volume of the porous medium for the system of interest (L^3), m is the mass of NAPL (M), a is the specific interfacial area between the NAPL and the aqueous phase (L^{-1}) and K_L is the mass transfer rate coefficient (T^{-1}). Then eqn.(2.1) can be rewritten as;

$$\dot{M} = K_L(C_s - C_a) \tag{2.3}$$

Miller *et al.* [20] performed column experiments to calculate the mass transfer rate coefficient from an analytical solution for the steady state condition of an advective-dispersive -reactive (ADR) equation subject to

$$C(0) = 0 \tag{2.4}$$

$$\left.\frac{\partial C}{\partial x}\right|_{x=\infty} = 0 \tag{2.5}$$

The effluent concentrations from the column packed with glass beads and DNAPL were measured at different aqueous phase velocities and different NAPL saturation.

Then, the mass transfer rate coefficient was calculated as a function of effluent concentration from the steady state solution of Van Genuchten and Alves [31];

$$\frac{C(x)}{C_s} = 1 - exp\left[(\frac{x}{2D_L})(v_x - \sqrt{v_x^2 + 4D_L K_L})\right] \tag{2.6}$$

where D_L is the coefficient of hydrodynamic dispersion in the x-direction ($L^2 \cdot T^{-1}$), v_x is the mean pore velocity in x-direction ($L \cdot T^{-1}$), $C(x)$ is the effluent concentration and C_s is the solubility concentration ($L^3 \cdot T^{-1}$). From this study, is was concluded that the calculated mass transfer rate coefficient increased as the NAPL saturation increased but there was no strong indication that the particle size influenced the mass transfer rate coefficient.

Dimensional analysis is a useful method widely used to generalise experimental results by forming a dimensionless parameters. The relationships among the dimensionless parameters improves the understanding and prediction of physical problems with the geometric similarity. Several correlation equations for the mass transfer coefficient have been formulated using dimensional analysis. The procedure is to incorporate the mass transfer coefficient into a dimensionless parameter called Sherwood number. The Sherwood number is a measure of the rates of interphase mass transfer and molecular diffusion [23].

$$Sh = \frac{k_l l_c}{D_m} = f(Re, Sc) \tag{2.7}$$

where Sh is a Sherwood number, Re is a Reynolds number, Sc is a Schmidt number, k_l is the mass transfer coefficient ($L \cdot T^{-1}$), l_c is a characteristic length (L), and D_m is the molecular diffusion in the aqueous phase($L^2 \cdot T^{-1}$).

$$Sc = \frac{\mu_a}{\rho_a D_m} \tag{2.8}$$

where μ_a is the dynamic viscosity in aqueous phase ($M \cdot L^{-1}4 \cdot T^{-1}$), and ρ_a is the density of the aqueous phase ($M \cdot L^{-3}$).

Since the mass transfer rate coefficient will be used instead of the mass transfer coefficient Miller *et al.* [20] proposed an empirical relation between a modified Sherwood number and the mass transfer rate coefficient.

$$Sh' = \frac{K_L d_p^2}{D_m} \tag{2.9}$$

where Sh' is a modified Sherwood number, d_p is the diameter of the porous media particle (L), and D_m is the molecular diffusion in the aqueous phase ($L^2 \cdot T^{-1}$). This modified Sherwood number is used in the study of pore-scale dissolution. For field-scale dissolution, Sale and McWhorter [27] defined a macroscopic Sherwood number as;

$$Sh_m = \frac{K_L L^2}{D_L \phi} \tag{2.10}$$

where Sh_m is a macroscopic Sherwood number, L is the length of a DNAPL subzone measured in the direction of the aqueous phase flow (L), D_L is the longitudinal dispersion coefficient ($L^2 \cdot T^{-1}$) and ϕ is porosity.

Miller *et al.* [20], Powers *et al.* [23] and Imhoff *et al.* [15] used their experimental data from one dimensional experiments to establish the correlation of the modified Sherwood number with the Reynolds number and the Schmidt number. These correlation were developed using different NAPLs and various Reynold numbers and NAPL saturation. All of these experiments were done with relatively low NAPL saturations which were in the range 0.04-0.1. Miller *et al.* [20], and Powers *et al.* [23] concluded that the mass transfer rate is directly related to the aqueous phase velocity and Imhoff *et al.* [15] also concluded that the mass transfer rate coefficient is a function of the Darcy velocity.

Kim and Chrysikopoulos [16] developed a Sherwood number correlation for single component NAPL pools from a three-dimensional contaminant transport model. The mass transfer coefficient is estimated by a finite difference numerical method. It also

results in a mass transfer rate that is related to the groundwater velocity.

Saba and Illangasekare [26] performed experiments on the NAPL dissolution in two-dimensional flow field in sand to develop the modified Sherwood equation. They concluded that the mass transfer rate coefficient resulting from their Sherwood equation gives lower mass transfer rates than from the mass transfer rate coefficient estimated from the Sherwood equations determined in the one-dimensional flow experiments. The difference between those two methods of establishing the Sherwood equation is that in this two-dimensional set-up, the flow can by-pass over the contaminated pool while the earlier experiments in the one-dimensional flow done by others (Miller *et al.* [20], Powers *et al.* [23], Imhoff *et al.* [15], and , Powers *et al.* [24]), water is forced through the pool. Sherwood equation by Saba and Illangasekare is;

$$Sh = 11.34 Re^{0.2767} Sc^{0.3} \left[\frac{d_{50}\phi_n}{\tau L} \right]^{1.037} \tag{2.11}$$

where Sh is the Sherwood number, Re is the Reynold number, Sc is the Schmidt number, d_{50} is the mean particle diameter (L), ϕ_n is the initial volumetric NAPL content of the source, τ the is tortuosity of sand, and L is the path length inside the contaminant zone (L).

Even though the correlations that appear in the literature are quite different from each other, the numerical study by Mayer and Miller [19] showed that the rate of mass removal in a homogeneous porous medium was rather insensitive to the correlation used.

Zhu and Sykes [33] used a numerical model to examine the NAPL dissolution process. They suggested that the mass transfer rate coefficient obtained from one-dimensional column experiments might be unsuitable for use in the field-scale dissolution. It should be noted here that the mass transfer rate coefficient reported in the literatures is in the range of 100-1000 day^{-1} (Miller *et al.* [20], Imhoff *et al.* [15]).

They also added that a constant mass transfer rate coefficient is unsuccessful for prediction of the observed decrease of the mass transfer rate over time. Consequently the decline in effluent concentration cannot be predicted. They recommended that the importance of problem scale be investigated in order to understand the NAPL dissolution process.

2.4 The dissolution of single DNAPL

Sale and McWhorter [27] used an analytical technique with spatial superposition to estimate the steady state mass transfer rate from the single component DNAPL source zone. With the spatial superposition method, the mass transfer from each subzone in the complex source zone can be calculated.

The concentration at the center of the jth subzone (x_j, y_j, z_j) resulting from the steady state mass transfer from N subzones is;

$$C_a(x_j, y_j, z_j) = \sum_{i=1}^{N} K_L(C_s - C_a(x_i, y_i, z_i) F(x_j - x_i, y_j - y_i, z_j - z_i) \tag{2.12}$$

where i,j = 1,2,...,N

$$F(x, y, z) = \frac{1}{\phi} \int_0^{\infty} F_x(x, t) F_y(y, t) F_z(z, t) \tag{2.13}$$

$$F_x(x, t) = \frac{1}{2} \left[\mathrm{erf}\left(\frac{x + a - v_w t}{2\sqrt{D_L t}}\right) - \mathrm{erf}\left(\frac{x - a - v_w t}{2\sqrt{D_L t}}\right) \right] \tag{2.14}$$

$$F_y(y, t) = \frac{1}{2} \left[\mathrm{erf}\left(\frac{y + b}{2\sqrt{D_T t}}\right) - \mathrm{erf}\left(\frac{y - b}{2\sqrt{D_T t}}\right) \right] \tag{2.15}$$

$$F_z(z, t) = \frac{1}{2} \left[\mathrm{erf}\left(\frac{z + c}{2\sqrt{D_T t}}\right) - \mathrm{erf}\left(\frac{z - c}{2\sqrt{D_T t}}\right) \right] \tag{2.16}$$

where x is the direction of the groundwater flow, y and z are the horizontal and the vertical directions, a, b, c are the half length, width and height of the subzone, D_L is the longitudinal dispersion coefficient ($\mathrm{L^2 \cdot T^{-1}}$), D_T is the transverse dispersion coefficient ($\mathrm{L^2 \cdot T^{-1}}$), and v_w is the seepage velocity ($\mathrm{L \cdot T^{-1}}$)

Eqn.(2.12) was written for N subzones resulting in a set of N equations with N concentration unknowns. The matrix equation used to solve for the concentrations is;

$$\boldsymbol{C_a} = C_s([\boldsymbol{F}] + K_L^{-1}[\boldsymbol{I}])^{-1} \cdot [\boldsymbol{F}]\boldsymbol{U} \tag{2.17}$$

where $\boldsymbol{C_a}$ is an N component vector of concentrations at the geometric centers of the subzones, $[\boldsymbol{F}]$ is an N by N matrix of transport constraint functions, $[\boldsymbol{I}]$ is an N by N identity matrix, and $\boldsymbol{U}$ is an N component vector of unit values (the unity vector).

They found that rate-limited mass transfer at the field-scale resulted basically from the advective-dispersive transport in the aqueous phase as characterised by the matrix [F]. The effect of the mass transfer rate coefficient as characterized by the matrix K_L^{-1}[I], has only a small effect on over all mass transfer. From their model, it was concluded that most of the mass transfer occurs at the leading edge of the source zone which results in the reduction of the perimeter of DNAPL subzones. However, the reduction in the DNAPL saturation will be small. Mass transfer rate and the time of mass transfer from each subzone are a function of the subzone geometry and the direction and magnitude of the groundwater flow. Using their solution to model the multiple subzones, they found that mass transfer rates of subzones located downgradient from another subzone are reduced due to effects of the mass transfer rate of the upgradient subzone. This leads to the conclusion that removing subzones that are either affected by upgradient subzones or have effect on downgradient subzones may have little effect on the overall mass transfer rate from the source zone.

2.5 Dissolution of multicomponent DNAPLs

DNAPLs that have been observed in groundwater mostly are mixtures. Thus, the dissolution of multicomponent DNAPLs will be considered in this research. Banerjee [3] presented the equation that governs the equilibrium dissolution of organic mixtures in water.

$$\frac{C^a}{C^a_{sol}} = \frac{(X^a)_{org}(\gamma^a)_{org}(\gamma^a)^p_{aq}}{(\gamma^a)_{aq}} \tag{2.18}$$

where C^a is the aqueous concentration of component a, C^a_{sol} is the aqueous solubility of pure component a, $(X^a)_{org}$ is the mole fraction of component a in the non-aqueous organic phase, $(\gamma^a)_{org}$ and $(\gamma^a)_{aq}$ are the activity coefficients in the organic phase and the aqueous phase, respectively. $(\gamma^a)^p_{aq}$ is the activity coefficient of the pure component in water.

Assumptions presented by Shiu *et al.* [30] and Mackay *et al.* [18] are;

- There are no chemical interactions or small interactions between components in the aqueous phase. That is $(\gamma^a)^p_{aq}$ is equal to $(\gamma^a)_{aq}$.
- There are no chemical interactions or interactions are assumed to be insignificant between components of similar chemical structure in the organic phase such as chlorinated solvents or chlorinated benzenes. That is $(\gamma^a)_{org}$ equals 1. Or it can be said that compounds in the organic phase have an ideal behavior.

With the assumptions, eqn.(2.18) is reduced to (in this case the organic phase is substituted by the NAPL phase);

$$C^a_{eff} = X_a C^a_{sol} \tag{2.19}$$

If there are n components in the DNAPL, n equations of eqn.(2.19) can be written to obtain the effective solubility for each component. Eqn.(2.19) is analogous to

Raoult's law for the vapor phase and is often considered as Raoult's law for the aqueous phase.

Broholm and Feenstra [4] showed experimentally that binary and ternary mixtures of NAPL follow almost ideal behavior. This experiment supports the approximation that $(\gamma^a)_{org}$ equals 1. And for first assumption is true for petroleum hydrocarbons and chlorinated solvent which have relatively low solubility resulting in low concentration and, hence, little interactions in the aqueous phase [9].

Chrysikopoulos and Lee [7] used a semi-analytical method to model the dissolution of a multicomponent NAPL pool. The analytical solution used in their work was derived by Chrysilkopoulos [6] for the three-dimensional transient contaminant transport from rectangular, elliptic and circular pools. In this solution, the thickness is assumed to be insignificant relative to the thickness of the aquifer. The NAPL dissolution is described by the mass transfer relationship at the NAPL-water interface as;

$$D_e \frac{\partial C(t,x,y,0)}{\partial Z} = -k(t,x,y)[C_s - C(t,x,y,\infty)] \tag{2.20}$$

where D_e is the effective molecular diffusion coefficient ($L^2 \cdot T^{-1}$), $k(t,x,y)$ is the local mass transfer coefficient ($L \cdot T^{-1}$), C_s is the aqueous concentration at the interface ($M \cdot L^{-3}$) and $C(t,x,y,\infty)$ is the contaminant concentration outside the boundary layer and is consider to be zero. In this work, it is assumed that the local mass transfer coefficient is equal to the time invarient overall mass transfer coefficient, k^*.

$$k^* = k(t,x,y) \tag{2.21}$$

Then eqn.(2.20) becomes;

$$D_e \frac{\partial C(t,x,y,0)}{\partial Z} = -k^* C_s \tag{2.22}$$

This boundary condition indicates that the concentration at z=0 or at the macroscopic NAPL-water interface has a linear relationship with the Z-direction or the changes in

the concentration in the z-direction are constant. And since it is assumed that the thickness of the source is insignificant, it implies that there is no groundwater flow through the NAPL pool. All the dissolution occurs at the macroscopic NAPL-water interface only.

The shapes of the pool used in this calculation are those of the circle and the ellipse. The mass transfer relationship at the macroscopic water-NAPL interface is given by eqn.(2.20). But the aqueous concentration at the interface (C_s) has been replaced by the equilibrium aqueous solubility of any component p as;

$$D_e \frac{\partial C_p(t,x,y,0)}{\partial Z} = -k_p^*(C_p^w(t) - C_{b_p}) \tag{2.23}$$

$$C_p^w = C_{s_p} X_p(t) \gamma_p(X_p) \tag{2.24}$$

where D_e is the effective molecular diffusion coefficient ($L^2 \cdot T^{-1}$), k^* is the average mass transfer coefficient ($L \cdot T^{-1}$), C_p^w is the equilibrium aqueous solubility of component p ($M \cdot L^{-3}$), C_{s_p} is the single component aqueous solubility ($M \cdot L^{-3}$), X_p is the mole fraction of component p, γ_p is the dimensionless activity coefficient of component p, C_{b_p} is the background liquid phase solute concentration and in this calculation it is assumed to be 0, and C_p is aqueous phase solute concentration of component p ($M \cdot L^{-3}$).

They used their model to investigate the dissolution of the mixture of 1,1,1-TCA (solubility limit of 4.5 $kg \cdot m^{-3}$) and TCE (solubility limit of 1.1 $kg \cdot m^{-3}$) in pools with circular and elliptic shape. The results showed that the mass of 1,1,2-TCA dissolved faster than TCE leading to the lower mole fraction of 1,1,2-TCA and the higher mole fraction of TCE.

2.5.1 The effective solubility model

The effective solubility model (ESM) was developed by Feenstra [9]. It is used to estimate the change of the ratio of concentration released from multi-component DNAPLs. The aqueous concentration of each component can be determined by the amount of NAPL mass of each component using the Raoult's law. In ESM, the NAPL pool can be modelled by one cell or several cells. Clean water flows into the cell and equilibrium occurs. The NAPL phase mass dissolves into the aqueous phase mass and the sorbed-phase mass until equilibrium is achieved. The initial mass in each cell is assumed to be in the NAPL-phase. The mole fraction of that NAPL phase is used to calculate the aqueous concentration by Raoult's law. And then the sorbed-phase mass can be determined from the aqueous concentration. The aqueous-phase mass can also be determined from the aqueous concentration. Once the aqueous-phase mass and the sorbed-phase mass have been calculated, they can be added to the NAPL to get the total mass in each cell.

The sum of these three masses may exceed the initial total mass. In order to get an equilibrium among mass, a revision is needed. The NAPL phase mass is recalculated as the total mass minus the aqueous-phase mass and the sorbed-phase mass. Then the revised NAPL phase mass is used to recalculate the aqueous-phase concentration until it does not change significantly between iterations. Then equilibrium among the NAPL-phase, the sorbed-phase and the aqueous-phase mass has been achieved.

For one cell, the new total mass is used for the next step. For several cells, the aqueous-phase mass from the upgradient cell is moved down gradient and added to the NAPL-phase mass and the sorbed-phase mass resident in that down gradient cell. The results of this model are shown as the relationship between the NAPL phase mass remaining and the ratio of the concentration of the two NAPL components.

This model can be used without data on the geometry of NAPL source zone, groundwater flow rates or mass transfer coefficients. These conditions might cause some error in the estimation since Sale and McWhorter [27] suggested that the source zone architecture is a fundamental factor controlling the mass transfer rate and the longevity of the source zone. Miller *et al.* [20], and Powers *et al.* [23] concluded that the mass transfer rate is directly related to the aqueous phase velocity. Imhoff *et al.* [15] also concluded that the mass transfer rate coefficient is a function of the Darcy velocity.

CHAPTER 3

The transient state dissolution of DNAPLs

In this research, a semi-analytical solution is used to model the dissolution of a DNAPL source zone from a single component and a multi-component DNAPLs. One-dimensional flow under uniform and steady state and three-dimensional transport under transient state will be considered. The transient state condition will be considered because;

- The mass transfer rate is assumed to be changing with time.
- In the system with multicomponent DNAPLs, the dissolution process is also governed by the mole fraction of each component. As the dissolution processproceeds, mass will be depleted from the NAPL-phase. The changing in mass will also affect the mole fraction. Various mole fractions of each component will then affect the effective solubility. So it is important to monitor the changing in the mole fraction.

This research is an extension work from Sale and McWhorter [27] Their method is called Multiple Analytical Source Superposition Technique or MASST. Transient state is considered in this research, therefore this method is referred as TMASST for Transient Multiple Analytical Source Superposition Technique .

3.1 Interphase mass transfer

Consider a DNAPL in the groundwater at a macroscopic scale as shown in figure(3.1), as groundwater flows through the pore between the soil grain, it makes contact with the DNAPL. Since the incoming groundwater is free of the contaminant, its aqueous phase concentration is zero. This creates a non-equilibrium condition that drives NAPL dissolution. The concentration difference in the DNAPL and in the groundwater as a aqueous phase concentration is the driving force of the mass transfer. The transfer of mass will continue until the solute concentration in the aqueous phase is equal to the effective solubility.

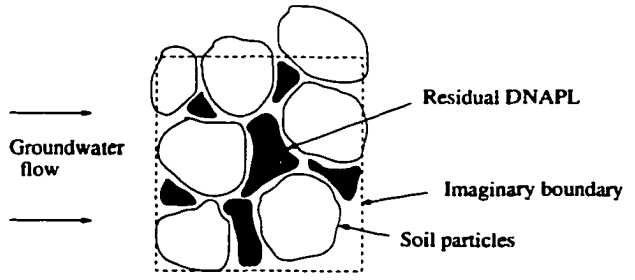

Figure 3.1: Macroscopic dissolution

The mass transfer rate of the DNAPL can be estimated by the stagnant film model [29] using eqn.(2.3). The mass transfer rate in this work will then be evaluated for the DNAPL source zone not at each DNAPL subzone. It is assumed that the mass transfer rate is constant within any considering source zone during a small time step. And the mass transfer rate is being calculated at the center of the source zone. The DNAPL saturation is relatively low so that the groundwater can flow into the DNAPL source zone.

3.2 The governing equation

When the mass being transferred from the NAPL phase into the aqueous phase, the dissolved mass will then be transported down gradient by the advective and diffusive forces. Consider a DNAPL pool in the saturated zone with a uniform groundwater flow through the pool, as shown in figure (3.2).

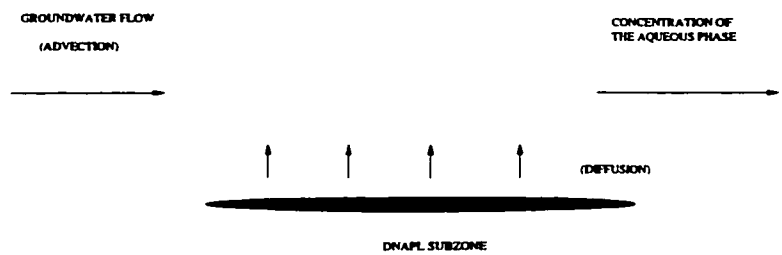

Figure 3.2: Dissolution from a DNAPL pool

The partial differential equation that governs the transient transport from a dissolving DNAPL pool in three-dimensional homogeneous porous media under the steady state uniform groundwater flow is

$$\frac{D_{ij}}{R}\frac{\partial^2 C}{\partial x_i \partial x_j} - \frac{v_1}{R}\frac{\partial C}{\partial x_1} - \mu C = \frac{\partial C}{\partial t} \qquad \text{i,j} = 1,2,3 \tag{3.1}$$

where

$$D_{ij} = \begin{bmatrix} D_{11} & D_{12} & D_{13} \\ D_{21} & D_{22} & D_{23} \\ D_{31} & D_{32} & D_{33} \end{bmatrix} \tag{3.2}$$

$$D_{11} = \alpha_L v_{x_1} + D^* \tag{3.3}$$

$$D_{22} = D_{33} \tag{3.4}$$

$$= \alpha_T v_{x_1} + D^* \tag{3.5}$$

$$D_{ij} = 0 \qquad \text{when i} \neq \text{j} \tag{3.6}$$

where D_{ij} is the coefficient of hydrodynamic dispersion ($L^2 \cdot T^{-1}$), α_L is the longitudinal dynamic dispersivity (L), α_T is the transverse dynamic dispersivity (L), D^* is

the effective molecular diffusion ($L^2 \cdot T^{-1}$), ϕ is porosity, v is the average groundwater velocity ($L \cdot T^{-1}$), t is time (T), R is the retardation facter, C is the aqueous phase concentration ($M \cdot L^{-3}$), μ is the first-order decay coefficient and x_1, x_2 and x_3 are the space co-ordinates. It is assumed that x_1 is the direction of groundwater flow.

In this research, a linear isotherm is assumed to describe the retardation of the contaminant. The retardation factor (R) can be expressed as

$$R = 1 + \frac{\rho_b}{\phi} K_d \tag{3.7}$$

$$K_d = K_{oc} f_{oc} \tag{3.8}$$

where ρ_b is the bulk mass density of the porous media ($M \cdot L^{-3}$), ϕ is the porosity, K_d is the distribution coefficient ($L^3 \cdot M^{-1}$), K_{oc} is the soil sorption coefficient or the soil organic carbon partition coefficient ($L^3 \cdot M^{-1}$) which is used to estimate the partitioning of an organic chemical between soil and the aqueous solution, f_{oc} is the organic carbon fraction (dimensionless).

To estimate the rate of the degradation of a chemical, a simple first-order equation is assumed. The first-order decay coefficient is estimated from the half life:

$$\mu = \frac{0.693}{t_{0.5}} \tag{3.9}$$

where $t_{0.5}$ is the half life of chemicals (T), and μ is the first-order decay coefficient (T^{-1}).

Assumptions used in this research to simplify the problem are;

- Groundwater flow is uniform and steady state.
- DNAPLs are present in the saturated zone.
- The porous media is isotropic and homogeneous.
- Transverse dispersion and longitudinal dispersion are constant.

- DNAPLs applicable in this research are chemicals which are satisfied assumptions in the section 2.5.

B. Hunt [13] presented solutions of the dispersion equation for instantaneous point, line and plane sources through analogy to the equations of heat conduction [2].

The initial condition is that concentrations are zero everywhere except at the origin.

$$C(x_1, x_2, x_3, 0) = 0 \quad x_1, x_2, x_3 \neq 0$$

And the initial distribution of concentration is approximated with the Dirac delta function.

$$M_o = \int_{-\infty}^{\infty} \int_{-\infty}^{\infty} \int_{-\infty}^{\infty} C(x_1, x_2, x_3, 0) \phi dx_1 dx_2 dx_3$$

The fundamental solution for an instantaneous point source is;

$$C(x_1, x_2, x_3, t) = \frac{M_o}{\phi} f_1(x_1, t) f_2(x_2, t) f_3(x_3, t) \tag{3.10}$$

where M_o is the mass release (M), ϕ is the porosity and the dimension of the f-function is $L^{-1}$and

$$\begin{aligned} f_1(x_1, t) &= \frac{1}{2\sqrt{\pi D_{11} t/R}} \exp\left[\frac{-(x_1 - v_1 t/R)^2}{4D_{11} t/R} - \mu t\right] \\ f_2(x_2, t) &= \frac{1}{2\sqrt{\pi D_{22} t/R}} \exp\left(\frac{-x_2^2}{4D_{22} t/R}\right) \\ f_3(x_3, t) &= \frac{1}{2\sqrt{\pi D_{33} t/R}} \exp\left(\frac{-x_3^2}{4D_{33} t/R}\right) \end{aligned}$$

To obtain the solution for continuous mass release in a prism shown in figure (3.3) which the instantaneous point source solution, eqn.(3.10), is integrated over a finite volume. The L_1, L_2, and L_3 are the half length, height and width of the source prism

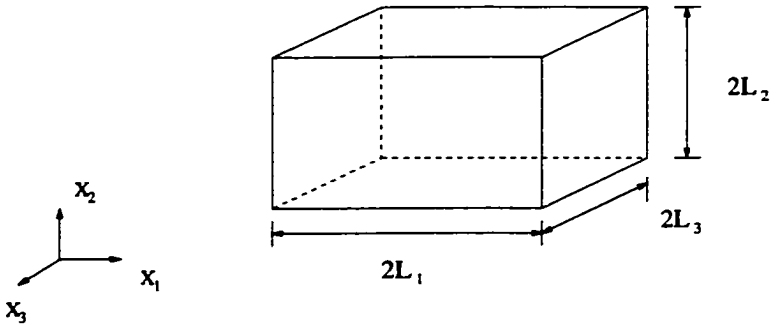

Figure 3.3: A DNAPL pool in the groundwater

(L). The details of obtaining the solution for continuous mass release in a prism are presented in Appendix A. The result is;

$$C(x_1, x_2, x_3, t) = \frac{1}{\phi} \int_0^t \frac{dM_3}{d\tau} F_1(x_1, t-\tau) F_2(x_2, t-\tau) F_3(x_3, t-\tau) d\tau \qquad (3.11)$$

where $\frac{dM_3}{d\tau}$ is the mass transfer rate or $\dot{M}$ ($\mathrm{M \cdot L^{-3} \cdot T^{-1}}$), M_3 is the mass released per unit volume of porous medium and the dimensionless F-functions are

$$F_1(x_1, t) = \frac{e^{-\mu t}}{2} \left[\mathrm{erf}\left(\frac{x_1 + L_1 - v_1 t/R}{2\sqrt{D_{11} t/R}}\right) - \mathrm{erf}\left(\frac{x_1 - L_1 - v_1 t/R}{2\sqrt{D_{11} t/R}}\right) \right] \qquad (3.12)$$

$$F_2(x_2, t) = \frac{1}{2} \left[\mathrm{erf}\left(\frac{x_2 + L_2}{2\sqrt{D_{22} t/R}}\right) - \mathrm{erf}\left(\frac{x_2 - L_2}{2\sqrt{D_{22} t/R}}\right) \right] \qquad (3.13)$$

$$F_3(x_3, t) = \frac{1}{2} \left[\mathrm{erf}\left(\frac{x_3 + L_3}{2\sqrt{D_{33} t/R}}\right) - \mathrm{erf}\left(\frac{x_3 - L_3}{2\sqrt{D_{33} t/R}}\right) \right] \qquad (3.14)$$

Since the partial differential equation is linear, the fundamental solution can be superimposed over different times. Instead of integrating the F-function in eqn.(3.11) over the whole period of time, the concentration at any time t can be calculated by the summation of the integration of the F-function over small time steps. By dividing time into small time steps, mass can be considered to be released constantly over that small time step. Therefore, the mass transfer rate, which is a function of time, can be accommodated by this solution.

Later in this research, a pool of DNAPL will be divided into blocks, and multi-component DNAPLs will be considered. To avoid any confusion, from now on the

co-ordinate system will be rewritten as (x_1, x_2, x_3) rather (x, y, z) so that the subscript and the superscript for x, y, z can be used to indicate the number of the block, the component of DNAPL, and the number of the time step.

3.3 Solution for a single component DNAPL in a subzone

Mathematical model for a single component DNAPL in a subzone will be first considered. To start off with this simplest possible scenario at the contaminant site is because

- The mathematical model will be a fundamental procedure to the more complex situation later.
- This case will be used to compare against the more complex case whether the concentration, the mass transfer rate and the remaining mass in a single component DNAPL are different from a multicomponent DNAPL case.

A single component DNAPL is assumed to present in a DNAPL subzone dimensions of $2L_1 \cdot 2L_2 \cdot 2L_3$(figure(3.4)). The center of the released mass is at (x', y', z').

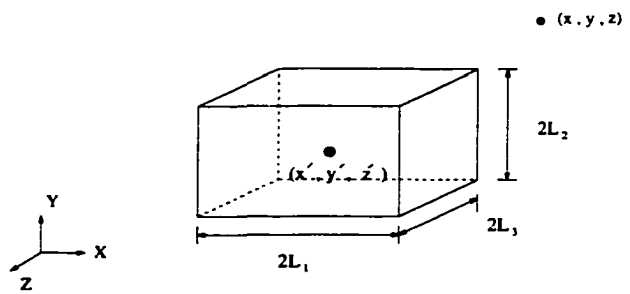

Figure 3.4: A block of DNAPL with a single component

The general equation for estimation of the dissolved aqueous concentration is;

$$C_a(x, y, z, t) = \frac{1}{\phi} \int_0^t \dot{M} F_1(x - x', t - \tau) F_2(y - y', t - \tau) F_3(z - z', t - \tau) d\tau \quad (3.15)$$

where

$$F_1(x-x',t) = \frac{e^{-\mu t}}{2}\left[\text{erf}(\frac{x-x'+L_1-v_1t/R}{2\sqrt{D_{11}t/R}}) - \text{erf}(\frac{x-x'-L_1-v_1t/R}{2\sqrt{D_{11}t/R}})\right]$$

$$F_2(y-y',t) = \frac{1}{2}\left[\text{erf}(\frac{y-y'+L_2}{2\sqrt{D_{22}t/R}}) - \text{erf}(\frac{y-y'-L_2}{2\sqrt{D_{22}t/R}})\right]$$

$$F_3(z-z',t) = \frac{1}{2}\left[\text{erf}(\frac{z-z'+L_3}{2\sqrt{D_{33}t/R}}) - \text{erf}(\frac{z-z'-L_3}{2\sqrt{D_{33}t/R}})\right]$$

At t = 0, the concentration in the groundwater or the concentration in the aqueous phase, C_a, equals zero since it is assumed that there is no contaminant in the groundwater initially. At t=t_1, some quantity of mass has been dissolved into the groundwater. It is assumed that t_1 is a very small time step. At the end of t_1, the average amount of mass released from the DNAPL zone between t=0 to t=t_1 can be calculated. And the mass transfer rate during t=0 - t_1 can be estimated. This mass transfer rate can be calculated using eqn.(2.1). The aqueous concentration, C_a and the equilibrium concentration, C_s at time=0 will be used to estimated the mass transfer rate during time = 0 - t_1. The general equation to calculate the mass transfer rate for component 1 at any time t can be written as;

$$\dot{M}^1_{t_i} = K_L(C^1_{s_{t_{i-1}}} - C^1_{a_{t_{i-1}}}) \tag{3.16}$$

where the superscript on $\dot{M}$, C_s and C_a indicate component 1 of the DNAPL and the subscript on $\dot{M}$, C_s and C_a indicate the time.

The mass transfer rate is calculated at the center of the block and is assumed to be constant for the whole block. Even though the mass transfer rates are changing with time, it is assumed to be constant over the small time step. In equation (3.15), the mass transfer rate therefore can be taken out of the integral. The mass transfer rate at any time t will affect the concentration not only at that particular time step but also at following times. To include these effects, superposition in time is applied

to estimate the concentration at any time t. After obtaining the mass transfer rate at any time t, the concentration at any time t can then be calculated. The process will go as;

$$\begin{aligned}
\dot{M}^1_{t_1} &= K_L(C^1_{s_{t_0}} - C^1_{a_{t_0}}) \\
C^1_{a_{t_1}}(x', y', z', t_1) &= \frac{\dot{M}^1_{t_1}}{\phi}\int_{t_0}^{t_1} \bar{F}_{t_1} d\tau \\
\dot{M}^1_{t_2} &= K_L(C^1_{s_{t_1}} - C^1_{a_{t_1}}) \\
C^1_{a_{t_2}}(x', y', z', t_2) &= \frac{\dot{M}^1_{t_1}}{\phi}\int_{t_0}^{t_1} \bar{F}_{t_2} d\tau + \frac{\dot{M}^1_{t_2}}{\phi}\int_{t_1}^{t_2} \bar{F}_{t_2} d\tau \\
&\vdots
\end{aligned}$$

where

$$\begin{aligned}
\bar{F}_{t_1} &= F_1(x' - x', t_1 - \tau)F_2(y' - y', t_1 - \tau)F_3(z' - z', t_1 - \tau) \\
\bar{F}_{t_2} &= F_1(x' - x', t_2 - \tau)F_2(y' - y', t_2 - \tau)F_3(z' - z', t_2 - \tau)
\end{aligned}$$

It is shown that the mass transfer rate is estimated at the beginning of each time step by eqn.(3.16). And it will be used to calculate the concentration of component 1 at the center of the block at any time t_i as;

$$C^1_{a_{t_i}}(x', y', z', t_i) = \frac{1}{\phi}\sum_{j=1}^{i} \dot{M}^1_{t_j}\int_{t_{j-1}}^{t_j} F_1(x' - x', t_i - \tau)F_2(y' - y', t_i - \tau)F_3(z' - z', t_i - \tau)d\tau \tag{3.17}$$

where i is the number of the time step.

It should be noted that the mass transfer rate which is released in the earlier time step will have the less effect on the concentration at the current time step. After the mass transfer rate of each time step is calculated, then the concentration at any co-ordinate in the groundwater system can be calculated by using that mass transfer rate. The F-function will indicate the effect of that mass transfer rate to the point where the concentration being calculated. Concentration at any (x, y, z) at any time

i of DNAPL component 1 can be written as;

$$C^1_{a_{t_i}}(x,y,z,t_i) = \frac{1}{\phi}\sum_{j=1}^{i} \dot{M}^1_{t_j} \int_{t_{j-1}}^{t_j} F_1(x-x',t_i-\tau)F_2(y-y',t_i-\tau)F_3(z-z',t_i-\tau)d\tau \tag{3.18}$$

Where i is the number of the time step.

Finally, the amount of mass loss after mass being transferred at each time step can be estimated from the mass transfer rate. Therefore, the remaining mass at the end of each time step can be calculated as:

$$\text{Mass}_{t_{i+1}} = \text{Mass}_{t_i} - \dot{M} \cdot 2L_1 \cdot 2L_2 \cdot 2L_3 \cdot \triangle t \tag{3.19}$$

3.4 Solution for a multi-component DNAPLs in a subzone

When there is more than one component DNAPL in the groundwater, the dissolution of the mixture will be governed by Raoult's law for the aqueous-phase (Banerjee [3]). At equilibrium, the aqueous concentration of each component will be the effective solubility instead of the solubility. The ability to dissolve mass is now controlled by the effective solubility. The effective solubility depends on the mole fraction and the solubility of each component. The mole fraction of each component is now another factor to regulate the mass transfer rate.

Consider a DNAPL subzone that contains a k species DNAPL. The mathematical solution to this problem is essentially the same as the one species of DNAPL. The difference is the equilibrium concentration or the effective solubility of each component has to be calculated from eqn. (2.19) at the beginning of each time step. The effective solubility depends on the remaining mole fraction after each dissolution process step.

The effective solubility will be used to calculate the mass transfer rate instead of the solubility as;

$$\dot{M}^k_{t_i} = K_L(C^k_{\text{eff}_{t_{i-1}}} - C^k_{a_{t_{i-1}}}) \tag{3.20}$$

where $\dot{M}^k_{t_i}$ is the mass transfer rate of component k at time t_i, $C^k_{\text{eff}_{t_{i-1}}}$ is the effective solubility of component k at time t_{i-1} and $C^k_{a_{t_{i-1}}}$ is the aqueous concentration of component k at time t_{i-1}.

Concentration at (x, y, z) at any time t_i of component k can be calculated as;

$$C^k_{a_{t_i}}(x,y,z,t_i) = \frac{1}{\phi}\sum_{j=1}^{i} \dot{M}^k_{t_j} \int_{t_{j-1}}^{t_j} F_1(x-x',t_i-\tau)F_2(y-y',t_i-\tau)F_3(z-z',t_i-\tau)d\tau \tag{3.21}$$

$$C^k_{a_{t_i}}(x,y,z,t_i) = \frac{1}{\phi}\sum_{j=1}^{i} \dot{M}^k_{t_j} \int_{t_{j-1}}^{t_j} F_1(x-x',t_i-\tau)F_2(y-y',t_i-\tau)F_3(z-z',t_i-\tau)d\tau$$

3.5 Solution for a multi-component DNAPLs in multiple subzones

DNAPL source zone in the groundwater are not continuously connected as shown in the figure (2.1). Mass released from an upstream pool has an influence on the mass transfer rate of the downstream pool. It can be hypothesised that the dissolution process of any DNAPL pool will effect the dissolution process of all other pools in the vicinity.

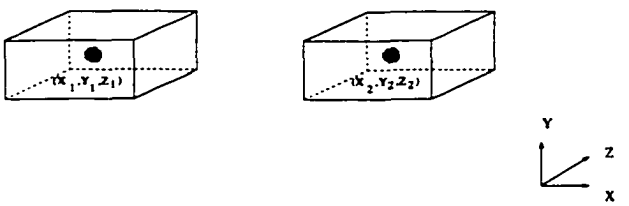

Figure 3.5: Two blocks of DNAPL with two components

Supposed there are two blocks of DNAPL, and each block contains a two-component DNAPL. The center of block 1 is at (x_1, y_1, z_1) and the center of block 2 is at (x_2, y_2, z_2) as shown in figure(3.5) The concentration of each component at the center of each subzone at time t_1 can be calculated as;

$$C^1_{a_{1_{t_1}}}(x_1,y_1,z_1,t_1) = \frac{1}{\phi}\left[\dot{M}^1_{1_{t_1}} \int_{t_0}^{t_1} \bar{F}^{11}_{t_1} d\tau + \dot{M}^1_{2_{t_1}} \int_{t_0}^{t_1} \bar{F}^{12}_{t_1} d\tau\right]$$

$$
\begin{aligned}
C^1_{a_{2_{t_1}}}(x_2,y_2,z_2,t_1) &= \frac{1}{\phi}\left[\dot{M}^1_{1_{t_1}}\int_{t_0}^{t_1}\bar{F}^{21}_{t_1}d\tau + \dot{M}^1_{2_{t_1}}\int_{t_0}^{t_1}\bar{F}^{22}_{t_1}d\tau\right]\\
C^2_{a_{1_{t_1}}}(x_1,y_1,z_1,t_1) &= \frac{1}{\phi}\left[\dot{M}^2_{1_{t_1}}\int_{t_0}^{t_1}\bar{F}^{11}_{t_1}d\tau + \dot{M}^2_{2_{t_1}}\int_{t_0}^{t_1}\bar{F}^{12}_{t_1}d\tau\right]\\
C^2_{a_{2_{t_1}}}(x_2,y_2,z_2,t_1) &= \frac{1}{\phi}\left[\dot{M}^2_{1_{t_1}}\int_{t_0}^{t_1}\bar{F}^{21}_{t_1}d\tau + \dot{M}^2_{2_{t_1}}\int_{t_0}^{t_1}\bar{F}^{22}_{t_1}d\tau\right]
\end{aligned}
$$

where the superscript on C_a and $\dot{M}$ indicate the DNAPL component and the subscript on C_a and $\dot{M}$ indicate the block number and;

$$
\begin{aligned}
\bar{F}^{11}_{t_1} &= F_1(x_1-x_1,t_1-\tau)F_2(y_1-y_1,t_1-\tau)F_3(z_1-z_1,t_1-\tau)\\
\bar{F}^{12}_{t_1} &= F_1(x_1-x_2,t_1-\tau)F_2(y_1-y_2,t_1-\tau)F_3(z_1-z_2,t_1-\tau)\\
\bar{F}^{21}_{t_1} &= F_1(x_2-x_1,t_1-\tau)F_2(y_2-y_1,t_1-\tau)F_3(z_2-z_1,t_1-\tau)\\
\bar{F}^{22}_{t_1} &= F_1(x_2-x_2,t_1-\tau)F_2(y_2-y_2,t_1-\tau)F_3(z_2-z_2,t_1-\tau)
\end{aligned}
$$

And at time t_2, the concentration at the center of each block is;

$$
\begin{aligned}
C^1_{a_{1_{t_2}}}(x_1,y_1,z_1,t_2) &= \frac{1}{\phi}\left[\dot{M}^1_{1_{t_1}}\int_{t_0}^{t_1}\bar{F}^{11}_{t_2}d\tau + \dot{M}^1_{2_{t_1}}\int_{t_0}^{t_1}\bar{F}^{12}_{t_2}d\tau + \dot{M}^1_{1_{t_2}}\int_{t_1}^{t_2}\bar{F}^{11}_{t_2}d\tau + \dot{M}^1_{2_{t_2}}\int_{t_1}^{t_2}\bar{F}^{12}_{t_2}d\tau\right]\\
C^1_{a_{2_{t_2}}}(x_2,y_2,z_2,t_2) &= \frac{1}{\phi}\left[\dot{M}^1_{1_{t_1}}\int_{t_0}^{t_1}\bar{F}^{21}_{t_2}d\tau + \dot{M}^1_{2_{t_1}}\int_{t_0}^{t_1}\bar{F}^{22}_{t_2}d\tau + \dot{M}^1_{1_{t_2}}\int_{t_1}^{t_2}\bar{F}^{21}_{t_2}d\tau + \dot{M}^1_{2_{t_2}}\int_{t_1}^{t_2}\bar{F}^{22}_{t_2}d\tau\right]\\
C^2_{a_{1_{t_2}}}(x_1,y_1,z_1,t_2) &= \frac{1}{\phi}\left[\dot{M}^2_{1_{t_1}}\int_{t_0}^{t_1}\bar{F}^{11}_{t_2}d\tau + \dot{M}^2_{2_{t_1}}\int_{t_0}^{t_1}\bar{F}^{12}_{t_2}d\tau + \dot{M}^2_{1_{t_2}}\int_{t_1}^{t_2}\bar{F}^{11}_{t_2}d\tau + \dot{M}^2_{2_{t_2}}\int_{t_1}^{t_2}\bar{F}^{12}_{t_2}d\tau\right]\\
C^2_{a_{2_{t_2}}}(x_2,y_2,z_2,t_2) &= \frac{1}{\phi}\left[\dot{M}^2_{1_{t_1}}\int_{t_0}^{t_1}\bar{F}^{21}_{t_2}d\tau + \dot{M}^2_{2_{t_1}}\int_{t_0}^{t_1}\bar{F}^{22}_{t_2}d\tau + \dot{M}^2_{1_{t_2}}\int_{t_1}^{t_2}\bar{F}^{21}_{t_2}d\tau + \dot{M}^2_{2_{t_2}}\int_{t_1}^{t_2}\bar{F}^{22}_{t_2}d\tau\right]
\end{aligned}
$$

where

$$
\begin{aligned}
\bar{F}^{11}_{t_2} &= F_1(x_1-x_1,t_2-\tau)F_2(y_1-y_1,t_2-\tau)F_3(z_1-z_1,t_2-\tau)\\
\bar{F}^{12}_{t_2} &= F_1(x_1-x_2,t_2-\tau)F_2(y_1-y_2,t_2-\tau)F_3(z_1-z_2,t_2-\tau)\\
\bar{F}^{21}_{t_2} &= F_1(x_2-x_1,t_2-\tau)F_2(y_2-y_1,t_2-\tau)F_3(z_2-z_1,t_2-\tau)\\
\bar{F}^{22}_{t_2} &= F_1(x_2-x_2,t_2-\tau)F_2(y_2-y_2,t_2-\tau)F_3(z_2-z_2,t_2-\tau)
\end{aligned}
$$

Generalising for N subzones, the concentration of component k at the center of any

subzone l at any time i can be calculated as;

$$C^k_{a_{t_i}}(x_l, y_l, z_l, t_i) = \frac{1}{\phi}\sum_{l=1}^{N}\sum_{j=1}^{i}\dot{M}^k_{l_{t_j}}\int_{t_{j-1}}^{t_j} F_1(x_m - x_l, t_i - \tau)F_2(y_m - y_l, t_i - \tau)F_3(z_m - z_l, t_i - \tau)d\tau \tag{3.22}$$

Where i is the time, N is the total number of DNAPL subzone, and l is the number of the block being considered, $(l = 1, \ldots, N)$.

3.6 Confirmation of the mathematical model

3.6.1 Comparison with the laboratory result

Whelan *et al.* [32] performed experiments on the dissolution of DNAPL in a two-dimensional sand aquifer. The DNAPL pool was placed at the bottom of the aquifer so that the pool would have a relatively flat surface. In this case, the groundwater flow would contact only the upper surface of the DNAPL pool. Holes were drilled in one of the tank's glass sides. These holes would serve as the sampling ports for the groundwater to be taken out to be analysed for dissolved phase DNAPL constituents later. The DNAPL used in this experiment was 1,1,2-trichloroethane (1,1,2-TCA). The groundwater velocity was 0.844 m·day^{-1}. Total time of collecting the groundwater sample was 195 hours. The experimental result used to compare with the mathematical model in this research is the concentration taken from port51 which located approximately 6.5 cm. above the end of the DNAPL pool from the tank bottom. Figure (3.6.1) shows the schematic diagram of the experimental setup.

In order to compare TMASST with the experimental results, the mathematical solution has to be adjusted to satisfy the same conditions as in the experiment set-up. In this experiment, the DNAPL pool can be viewed as a two-dimensional plane source. The solution to this problem can be derived from the instantaneous point source solution. To get a plane source solution, the instantaneous point sources

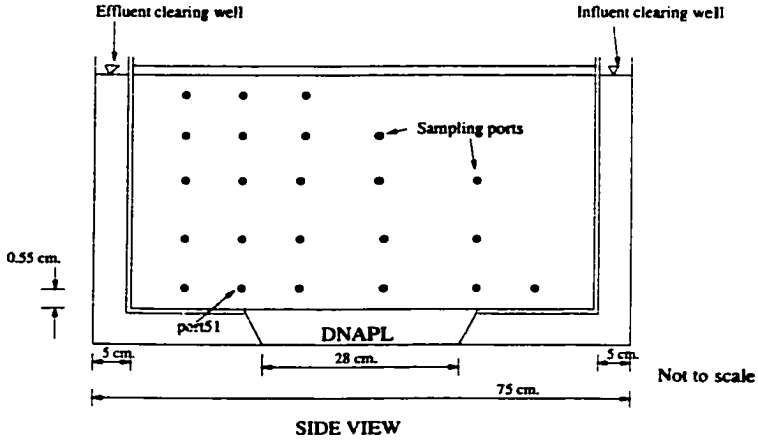

Figure 3.6: Schematic diagram of experimental set-up

solution is integrated over a finite plane; from $-L_1$ to L_1 in the x-direction and from $-L_2$ to L_2 in the y-direction where L_1 and L_2 are the half length of the size of the DNAPL pool in the x and y direction, respectively. Then the fundamental solution for the plane source solution is

$$\begin{aligned} C(x,y,z,t) &= \frac{\dot{M}_2}{\phi}\int_0^t\int_{-L_1}^{L_1}\int_{-L_2}^{L_2} f_1(x-x'\hat{x},t-\tau)f_2(y-y',t-\tau)f_3(z-z',t-\tau)dxdyd\tau \\ &= \frac{\dot{M}_2}{\phi}\int_0^t F_1(x-x',t-\tau)F_2(y-y',t-\tau)f_3(z-z',t-\tau)d\tau \end{aligned}$$

where $\dot{M}_2$ is the mass transfer rate per unit area, F_1 and F_2 are dimensionless and the dimension of f_3 is L^{-1} and

$$\begin{aligned} F_1(x,t) &= \int_{-L_1}^{L_1} f_1(x,t)dx \\ &= \frac{1}{2}\left[\mathrm{erf}\left(\frac{x+L_1-v_1t}{2\sqrt{D_Lt}}\right)-\mathrm{erf}\left(\frac{x-L_1-v_1t}{2\sqrt{D_Lt}}\right)\right] \\ F_2(y,t) &= \int_{-L_2}^{L2} f_2(y,t)dy \\ &= \frac{1}{2}\left[\mathrm{erf}\left(\frac{y+L_2}{2\sqrt{D_Tt}}\right)-\mathrm{erf}\left(\frac{y-L_2}{2\sqrt{D_Tt}}\right)\right] \\ f_3(z,t) &= \frac{1}{2\sqrt{\pi D_Tt}}\exp\left(\frac{-z^2}{4D_Tt}\right) \end{aligned}$$

In this experiment, only the upper surface of the DNAPL has contact with the groundwater. In TMASST, the DNAPL pool is assumed to have contact with the

groundwater in both the upper and lower surface. Therefore, the mass transfer rate estimated from TMASST is divided by two to get the only half of the mass transfer rate from the upper surface as in the experiment.

Table (3.1) shows the experimental data in this experiment. There are three parameters needed in TMASST but unavailable. The model was calibrated in order to get the best curve fitting graph. The calibrated parameters used in TMASST are shown in the table(3.2).

Condition	Experimental data
DNAPL	1,1,2-TCA
solubility limit ($kg \cdot m^{-3}$)	4.5
density ($kg \cdot m^{-3}$)	1439.0
pore velocity ($m \cdot day^{-1}$)	0.844
mass (kg)	0.711
sand porosity	0.46
sand bulk density ($g \cdot cm^{-3}$)	1.43
sand organic carbon (%)	0.00233
half life (year)	139.2

Table 3.1: Experimental data

Condition	parameters used in TMASST
K_L (day^{-1})	0.014
D_L ($m^2 \cdot day^{-1}$)	8.44×10^{-3}
D_T ($m^2 \cdot day^{-1}$)	1.688×10^{-4}

Table 3.2: Parameters used in TMASST

The mass transfer rate coefficient used in TMASST to fit the experimental results is relatively small compare to the value published in the literatures. The reason is that the mass transfer rate in the literatures were estimated from column experiments. The groundwater flow was forced through the DNAPL. While in this experiment, the groundwater had only the surface contact with the DNAPL.

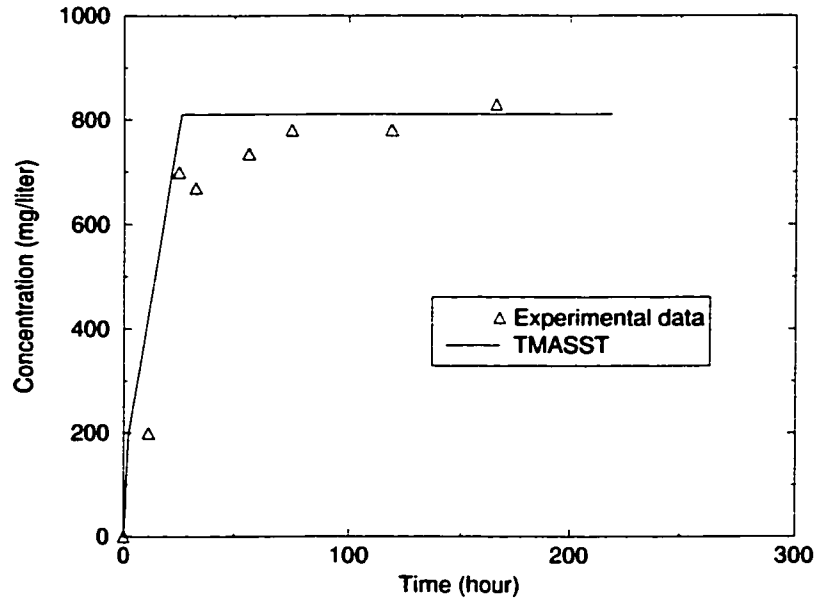

Figure 3.7: Comparison of concentration of 1,1,2-TCA between experiment and TMASST

The comparison result is shown in figure (3.7). There are number of parameters that are required in TMASST but not in the experiments. These may explain the difference between the experimental results and the result from TMASST. Calculated concentrations from TMASST reach steady state faster than the experimental concentrations. The laboratory results and the calculation from TMASST are considered acceptable.

3.6.2 Comparison with the plane source of constant concentration

In this case, an analytical solution by Hunt *et al.* [14] for the steady state advection-diffusion equation in a semi-infinite medium is used to assess TMASST. To choose this steady state to compare TMASST with is because there is no exact solution for the transient state to compare TMASST with. Solution by Sale and McWhorter [27] which is the steady state of MASST is also used for a comparison.

The governing equation for the steady state two-dimensional transport with one-

dimensional flow is

$$V_w \frac{\partial C_a}{\partial x} = D_T \frac{\partial^2 C_a}{\partial z^2} \quad \text{for x,z} > 0 \tag{3.23}$$

where x is the direction of the groundwater flow and z is the vertical direction. The boundary conditions are;

$$C_a(x, z = \infty) = 0 \tag{3.24}$$

$$C_a(x, z = 0) = C_s \quad 0 \leq \text{x} \leq \text{L} \tag{3.25}$$

$$C_a(x = 0, z) = 0 \tag{3.26}$$

The solution to the governing equation (3.23) subject to the above boundary conditions is

$$C_a(x, z) = C_s \left[1 - \text{erf} \left(\frac{z}{2\sqrt{D_T x / V_w}} \right) \right] \tag{3.27}$$

Sale and McWhorter [27] calculated the mass flux from the pool surface as a function of distance along the pool as;

$$J(x) = -\phi D_T \left. \frac{\partial C_a}{\partial z} \right|_{z=0} \tag{3.28}$$

$$= C_s \phi \sqrt{V_w D_T / x\pi} \tag{3.29}$$

where $J(x)$ is the mass flux from the pool into the aqueous phase flow ($\text{M}\cdot\text{L}^2\cdot\text{T}^{-1}$).

They estimated the mass transfer rate for this case as;

$$\dot{\mathbf{M}}_\mathbf{v} = C_s [F]^{-1} \mathbf{U} \tag{3.30}$$

where

$$F_{i,j} = \frac{1}{2\pi\phi\sqrt{D_T D_L}} \int_{x_i - x_j - a}^{x_i - x_j + a} \exp\left(\frac{V_w u}{2D_L}\right) K_0 \left(\frac{v_w u}{2D_L}\right) du \tag{3.31}$$

where $\dot{\mathbf{M}}_\mathbf{v}$ is an N component vector of mass transfer rate per unit volume from each subzone ($\text{M}\cdot\text{L}^{-3}\cdot\text{T}^{-1}$), $\mathbf{U}$ is the N component unit vector, F is an N by N matrix of

transport constraint functions and K_0 is the modified, zero order of Bessel function of the second kind and i, j = 1,2,...,N.

The conditions considered are $v = 10^{-5}$ m·sec^{-1}, $D_T = 10^{-9}$ m^2·sec^{-1}, $D_L = 10^{-8}$ m^2·sec^{-1} , $\phi = 0.3$, and $C_s = 1$ kg·m^{-3}. The plane source has been divided into equal strips as shown in figure(3.8).

In order to compare TMASST which calculate the transient state mass transfer rate, to the steady state solution by Hunt *et al.* [14] and MASST for the steady state solution by Sale and McWhorter [27], the program is run until concentrations reach the steady state or the change in concentrations is insignificant.

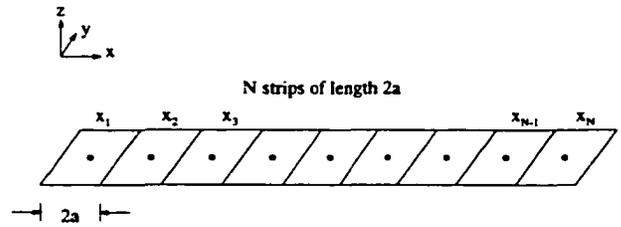

Figure 3.8: Concept of a segmented plane source

To get a plane source solution, an instantaneous point source solution is integrated over the finite length from $-L_1$ to L_1 in the x-direction and from $-\infty$ to ∞ in the y-direction since it is assumed that the plane is lined infinity in the y-direction.

The fundamental solution for the plane source is;

$$\begin{aligned} C(x,y,z,t) &= \frac{\dot{M}_2}{\phi}\int_0^t\int_{-L_1}^{L_1}\int_{-\infty}^{\infty} f_1(x-x',t-\tau)f_2(y-y',t-\tau)f_3(z-z',t-\tau)dxdyd\tau \\ &= \frac{\dot{M}_2}{\phi}\int_0^t F_1(x-x',t-\tau)f_3(z-z',t-\tau)d\tau \end{aligned}$$

where $\dot{M}_2$ is the mass transfer rate per unit area and

$$\begin{aligned} F_1(x,t) &= \int_{-L_1}^{L_1} f_1(x,t)dx \\ &= \frac{1}{2}\left[\text{erf}\left(\frac{x+L_1-v_1t}{2\sqrt{D_Lt}}\right) - \text{erf}\left(\frac{x-L_1-v_1t}{2\sqrt{D_Lt}}\right)\right] \end{aligned}$$

$$
\begin{aligned}
F_2(y,t) &= \int_{-\infty}^{\infty} f_2(y,t)dy \\
&= 1 \\
f_3(z,t) &= \frac{1}{2\sqrt{\pi D_T t}} \exp\left(\frac{-z^2}{4D_T t}\right)
\end{aligned}
$$

The comparison between the steady state MASST, the analytical solution and TMASST is shown in figure(3.9). It shows that TMASST gives a very close solution to the analytical solution and the steady state MASST.

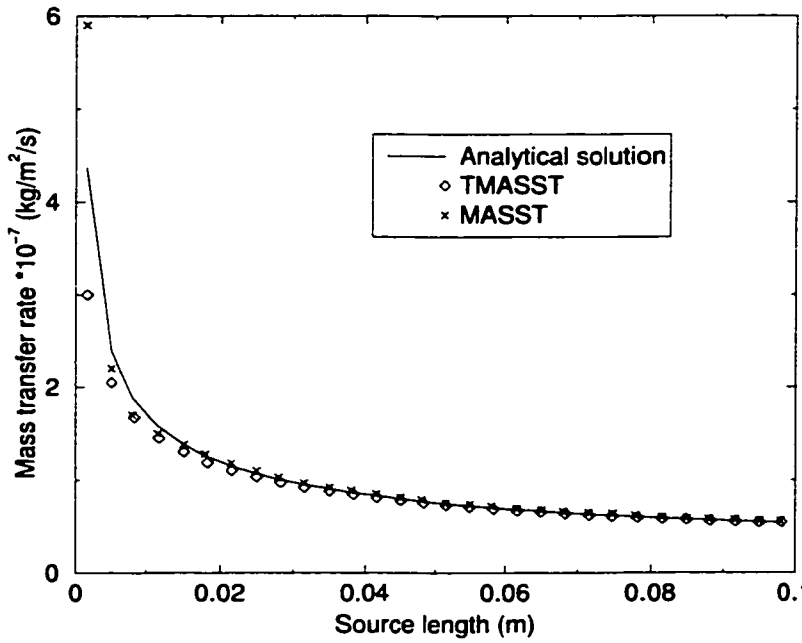

Figure 3.9: The mass transfer rate along the source length

CHAPTER 4

The field-scale mass transfer rate coefficient

Different scales of the dissolution process may be considered; the microscopic-scale, macroscopic-scale and field-scale. The dissolution is examined at the NAPL-water interface at the microscopic-scale. Therefore, the NAPL-aqueous phase interfacial area is needed. Recognising the difficulty of measuring the NAPL-aqueous phase interfacial area, many researchers studied the dissolution at the laboratory scale or the macroscopic-scale. At the macroscopic-scale, the NAPL-aqueous phase interfacial area can be ignored by using the mass transfer rate coefficient which is a parameter that lumps the mass transfer coefficient and the NAPL-aqueous phase interfacial area together. For the field-scale dissolution, the dissolution from several subzones in a source zone will be considered. Figure (4.1) shows the field-scale and macroscopic-scale dissolution.

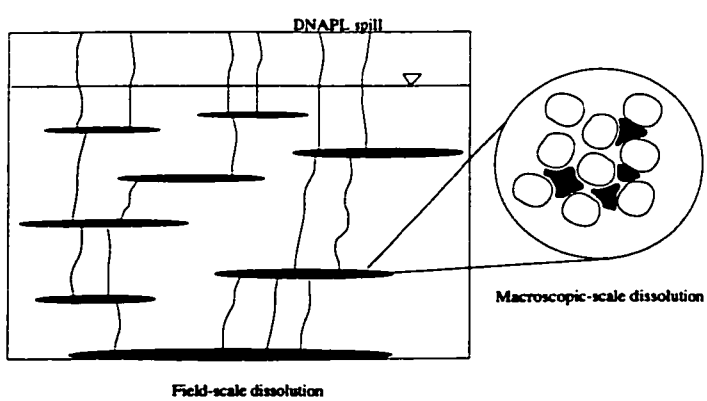

Figure 4.1: Field-scale and macroscopic-scale dissolution

The mathematical solution developed in chapter 3 can be used to estimated the field-scale mass transfer rate which is released from a DNAPL source zone. In order to estimate the field-scale mass transfer rate, the location and geometry of each subzone are required. However, the data are unavailable with the present technology. Without knowledge of the location and geometry of DNAPL subzones, the DNAPL source zone can be treated as a block of DNAPL. In doing so, a new parameter called the field-scale mass transfer rate coefficient is developed. The field-scale mass transfer rate coefficient will incorporate the complex part of location and geometry of DNAPL subzones. To handle the DNAPL source zone as one block gives another advantage which is less computational time. As shown in chapter3 in the section of solution for multi-component in multiple subzones, the mass transfer rate of each subzone will affect the concentration of any subzone. Therefore, the mass transfer rate of each subzone will be superimposed onto each other. This will give a rather long computational time.

Many researches studied NAPL dissolution at the laboratory scale or the macroscopic-scale (e.g. Miller *et al.* [20], Powers *et al.* [23], Imhoff *et al.* [15], Geller and Hunt [11], Whelan *et al.* [32] and Saba and Illangasekare [26]). Some studies were focused on NAPL pool dissolution such as Chrysikopoulos and Lee [7] and Sale and McWhorter [27]. Most of the mass transfer rate coefficient correlations have been established on the macroscopic scale (Miller *et al.* [20], Powers *et al.* [23], Imhoff *et al.* [15] and Saba and Illangasekare [26]). Kim and Chrysikopoulos [16] developed a mass transfer coefficient correlation for the DNAPL pool. Zhu and Sykes [33] suggested that the use of the mass transfer rate coefficient correlation developed from small laboratory experiments for the field-scale system should be done with caution. They concluded that the mass transfer rate coefficient correlation at the field-scale requires further

study.

In this chapter, a field-scale mass transfer rate coefficient will be developed. Several subzones will be randomly located into a source zone. The macroscopic mass transfer rate coefficient will be assigned to each subzone. Using the steady state MASST by Sale and McWhorter [27], the mass transfer rate of each subzone and the total mass transfer rate of the source zone can be estimated. This total mass transfer rate of the source zone can then be used to back calculate the field-scale mass transfer rate coefficient.

At steady state the concentration at the center of a single isolated subzone can be calculated from;

$$C_a(x,y,z,t) = \frac{1}{\phi}\int_0^\infty \dot{M}_v F_1(x-x',t)F_2(y-y',t)F_3(z-z',t)dt \tag{4.1}$$

where

$$\begin{aligned}
F_1(x-x',t) &= \frac{e^{-\mu t}}{2}\left[\mathrm{erf}(\frac{x-x'+L_1-v_1t/R}{2\sqrt{D_{11}t/R}}) - \mathrm{erf}(\frac{x-x'-L_1-v_1t/R}{2\sqrt{D_{11}t/R}})\right] \\
F_2(y-y',t) &= \frac{1}{2}\left[\mathrm{erf}(\frac{y-y'+L_2}{2\sqrt{D_{22}t/R}}) - \mathrm{erf}(\frac{y-y'-L_2}{2\sqrt{D_{22}t/R}})\right] \\
F_3(z-z',t) &= \frac{1}{2}\left[\mathrm{erf}(\frac{z-z'+L_3}{2\sqrt{D_{33}t/R}}) - \mathrm{erf}(\frac{z-z'-L_3}{2\sqrt{D_{33}t/R}})\right]
\end{aligned}$$

The mass transfer rate at the center of the DNAPL subzone at steady state derived by Sale and McWhorter [27] is;

$$\dot{M}_v = \frac{C_s}{\frac{1}{K_L} + F_0} \tag{4.2}$$

where

$$F_0 = \frac{1}{\phi}\int_0^\infty F_1(0,t)F_2(0,t)F_3(0,t)dt \tag{4.3}$$

The DNAPL source zone is comprised of many blobs of DNAPL subzones which may be disconnected from one another. There are areas within the source zone which are free of DNAPL. The spatial superposition of the responses can be used to estimate the mass transfer rate of several DNAPL subzones. Sale and McWhorter [27] have initiated a mathematical model to account for the effect of the mass transfer rate from all other subzones in the DNAPL source zone onto any particular subzone.

The concentration at the center of the j th subzone (x_j, y_j, z_j) as the result of the steady state mass transfer from N subzones is;

$$C_a(x_j, y_j, z_j) = \sum_{i=1}^{N} K_L(C_s - C_a(x_i, y_i, z_i))F(x_j - x_i, y_j - y_i, z_j - z_i) \tag{4.4}$$

for $i, j = 1, 2, 3, \ldots, N$

Equation (4.4) gives the concentration at the center of each subzone. Sale and McWhorter [27] also derived the mass transfer rate of each subzone in the matrix equation as;

$$\dot{\boldsymbol{M}}_v = C_s([\boldsymbol{F}] + K_L^{-1}[\boldsymbol{I}])^{-1} \cdot \boldsymbol{U} \tag{4.5}$$

where $[\boldsymbol{F}]$ is an N by N matrix of transport constraint functions, $[\boldsymbol{I}]$ is an N by N identity matrix, $\boldsymbol{U}$ is an N by 1 vector of unit values (the unity vector), $\dot{\boldsymbol{M}}_v$ is an N by 1 vector of mass transfer rates per unit volume from the individual subzones. It should be noted that the mass transfer rate coefficient that is used in the eqn.(4.5)for estimating the mass transfer rate of each subzone is a macroscopic-scale value.

Then the total mass transfer rate of the source zone can be calculated as;

$$\dot{M}_T = \sum_{i=1}^{N} V_i \dot{M}_{v_i} \tag{4.6}$$

where $\dot{M}_T$ is the total mass transfer rate ($\mathrm{M \cdot T^{-1}}$), V_i is the volume of each subzone i, and N is the number of the subzones.

The total mass transfer rate of the source zone will be used to estimate the field-scale mass transfer rate coefficient. Recall the equation to calculate the mass transfer rate as;

$$\dot{M}_v = K_L[C_s - C_a] \tag{4.7}$$

To estimate the field-scale mass transfer rate coefficient, eqn.(4.7) will be used which is the same basic equation used to estimate the mass transfer rate of each subzone. The total mass transfer rate can also be evaluated as the amount of mass being carried across the cross sectional area which is perpendicular ot the groundwater flow. This can also be expressed in the equation of;

$$\dot{M}_T = C_a q L^2 \tag{4.8}$$

$$\left[\frac{Mass}{Time}\right] = \left[\frac{Mass}{\text{vol. of water}}\right]\left[\frac{\text{vol. of water}}{\text{cross sectional area*time}}\right][\text{cross sectional area}] \tag{4.9}$$

or

$$C_a = \frac{\dot{M}_T}{\phi v L^2} \tag{4.10}$$

The field-scale mass transfer rate or the total mass transfer rate of the source zone will be put into eqn.(4.7). The mass transfer rate in eqn.(4.7) is the mass being transfer per unit volume of porous medium. To get the field-scale mass transfer rate into eqn.(4.7), it will be divided by the volume of the source zone. From equation (4.7), the field-scale mass transfer rate coefficient can be estimated as;

$$\tilde{K}_L = \frac{\dot{M}_v}{C_s - Ca} \tag{4.11}$$

Substitute equation(4.10) into equation (4.11), the field-scale mass transfer rate is estimated as;

$$\tilde{K}_L = \frac{\dot{M}_T \phi v}{C_s \phi v L^3 - \dot{M}_T L} \tag{4.12}$$

4.1 Calculation of the field-scale mass transfer rate coefficient

In this section, field-scale mass transfer rate coefficients for some DNAPLs will be calculated. The DNAPLs which will be used as examples are 1,1,1-TCA (1,1,1-Trichloroethane or methyl chloroform), 1,1,2-TCA (1,1,2-Trichloroethane or Vinyl trichloride) and chloroform. The problem will be considered in three dimensions. The size of each subzone is 0.1×0.002×0.1 m. and the size of the source zone is 2.0×2.0×2.0 m. The DNAPL subzones will be randomly placed in the source zone. The number of subzones in the source zone will be varied to relate to the field-scale DNAPL saturation. The field-scale DNAPL saturation can be estimated as;

$$S_n = \frac{\text{Volume of DNAPL}}{\text{Volume of void}} \tag{4.13}$$

$$= \frac{\text{mass of DNAPL}}{\rho_{DNAPL} \cdot \phi \cdot \text{Volume of a source zone}} \tag{4.14}$$

where ρ_{DNAPL} is the density of a DNAPL.

To find mass of DNAPL in a source zone, the DNAPL masses of each subzone are summed. It is assumed that the DNAPL saturation in each subzone is equal one. This assumption is applicable in this case because it is found by Sale and McWhorter [27] that within the DNAPL subzone, mass transfer rates are not dependent on the DNAPL saturation. The DNAPL masses in a subzone and a source zone are;

$$\text{DNAPL mass in a subzone} = \rho_{DNAPL} \cdot \phi \cdot \text{Volume of a subzone} \tag{4.15}$$

$$\text{DNAPL mass in a source zone} = N \cdot \rho_{DNAPL} \cdot \phi \cdot \text{Volume of a subzone} \tag{4.16}$$

where N is the number of subzones.

Finally, the field-scale DNAPL saturation is

$$S_n = \frac{N \cdot \rho_{DNAPL}\phi \cdot \text{Volume of a subzone}}{\rho_{DNAPL} \cdot \text{Volume of a source zone}} \tag{4.17}$$

$$= \frac{N \cdot \text{Volume of a subzone}}{\text{Volume of a source zone}} \tag{4.18}$$

Two cases of groundwater velocity will be investigated. The first groundwater velocity is 0.1 m·day^{-1} with D_L of 0.01 m^2·day^{-1} and D_T of $1.035 \cdot 10^{-4}$ m^2·day^{-1}. And the other groundwater velocity is 0.01 m·day^{-1} with D_L of $1.06 \cdot 10^{-3}$ m^2·day^{-1} and D_T of $7.048 \cdot 10^{-6}$ m^2·day^{-1}.

The field-scale mass transfer rate coefficient of 1,1,1-TCA, 1,1,2-TCA and chloroform for v = 0.01 m·day^{-1} and v = 0.1 m·day^{-1} are shown in figures (4.2) and (4.3), respectively.

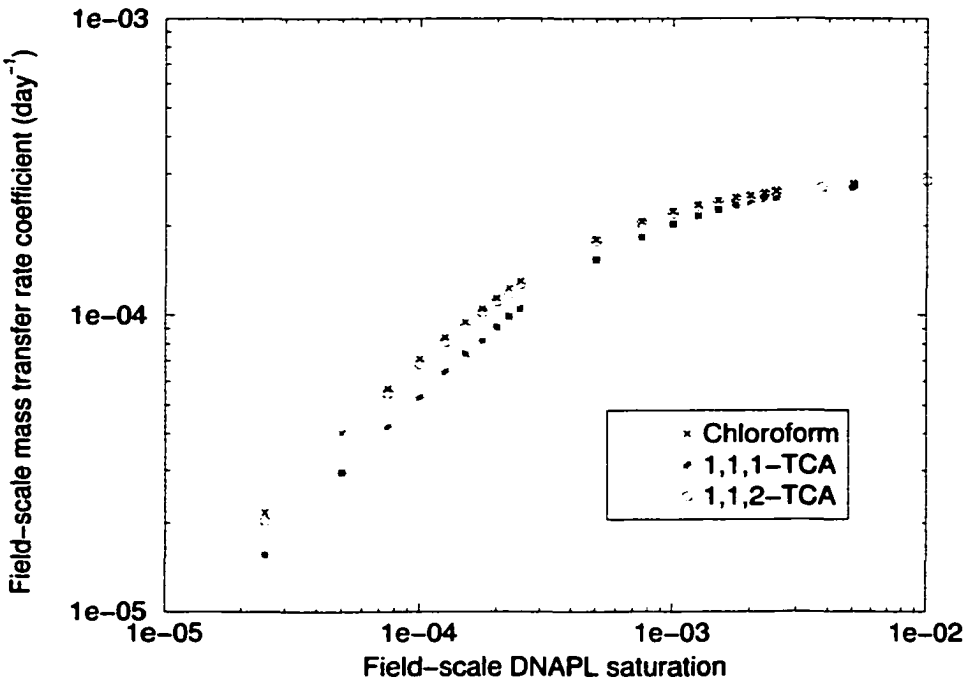

Figure 4.2: Field-scale mass transfer rate coefficient for v = 0.01 m/day

In both cases, the field-scale mass transfer rate coefficients change with the DNAPL saturation. The field-scale mass transfer rate coefficient tends to level off at the DNAPL saturation = 0.01 for v = 0.01 m·day^{-1} and at the DNAPL saturation = 0.001 for v = 0.1 m·day^{-1}. Chloroform and 1,1,2-TCA have similar values of field-scale mass transfer rate coefficients while 1,1,1-TCA gives lower field-scale mass transfer rate coefficients. Field-scale mass transfer rate coefficients for v = 0.1 m·day^{-1} are

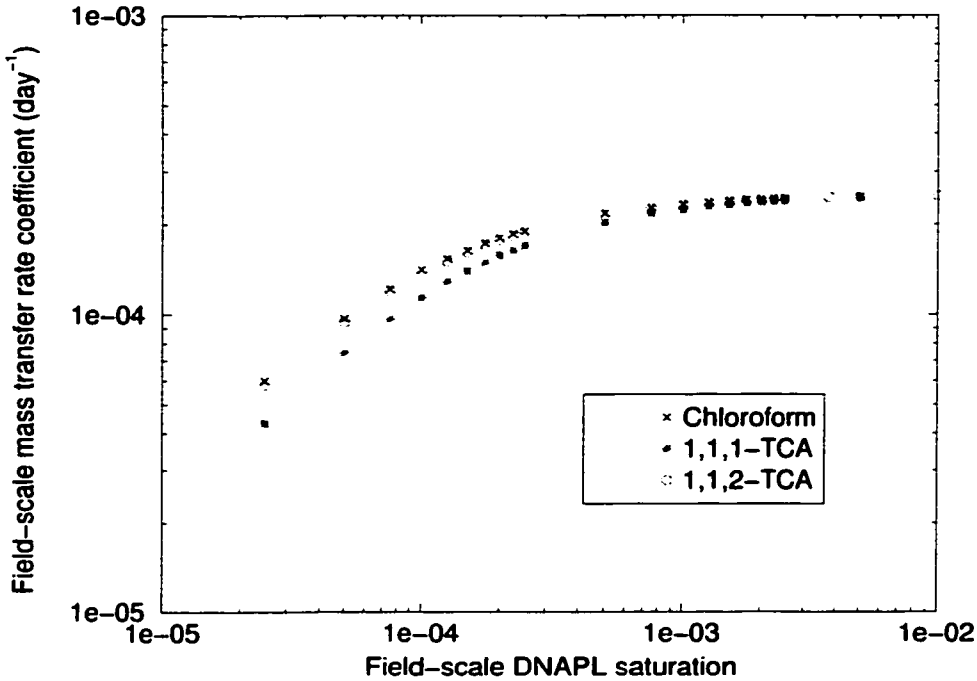

Figure 4.3: Field-scale mass transfer rate coefficient for v = 0.1 m/day

slightly higher than field-scale mass transfer rate coefficients for v = 0.01 m·day^{-1}. The field-scale mass transfer rate coefficient starts to decrease as the DNAPL saturation decreases. The maximum value of field-scale mass transfer rate coefficient in all cases are rather similar. This may suggested that the field-scale mass transfer rate coefficient is a function of the field-scale DNAPL saturation at low saturation.

CHAPTER 5

Case studies

In this chapter, the mathematical model developed in chapter 3 and the field-scale mass transfer rate coefficient estimated in chapter 4 will be used to investigate different scenarios of DNAPL dissolution. One, two and three components DNAPLs will be studied. The DNAPL selected as examples in these cases are contaminants that are commonly found in the groundwater. A computer code written in Fortran77 language will be used to calculate the mass transfer rate, the concentration, the mole fraction (in case of multi-component DNAPLs), and the remaining mass of the DNAPL.

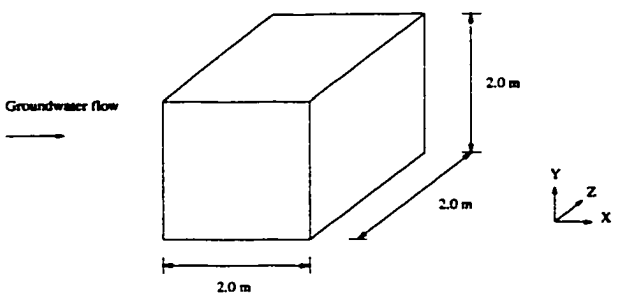

Figure 5.1: Geometry of DNAPL source zone for the case studies

In all of the following case studies, the physical settings for the DNAPL source zone is a rectangular box with the dimension of 2.0×2.0×2.0 m., figure (5.1). The analyses were performed in three dimensions. The source zone is assumed to be present in a sandy aquifer. The groundwater flow is uniform and under steady state with flow in the x-direction at the velocity of 0.1 m·day^{-1} and 0.01 m·day^{-1}. The co-

efficient of the longitudinal and the transverse hydrodynamic dispersion are 0.01 and $1.035 \cdot 10^{-4}$ $m^2 \cdot day^{-1}$ for the velocity of 0.1 $m \cdot day^{-1}$, respectively. And for the velocity of 0.01 $m \cdot day^{-1}$ the coefficient of the longitudinal and the transverse hydrodynamic dispersion are $1.06 \cdot 10^{-3}$ and $7.05 \cdot 10^{-5}$ $m^2 \cdot day^{-1}$, respectively. The porosity is 0.3. The initial field-scale DNAPL saturation is 0.03. The field-scale mass transfer rate coefficients used in the case studies are from the values estimated in chapter 4. The field-scale mass transfer rate coefficient has a piecewise linear relationship with the field-scale mass transfer rate coefficient. Relationships for each DNAPL component are shown in figures (5.2), (5.3), (5.4), and (5.5).

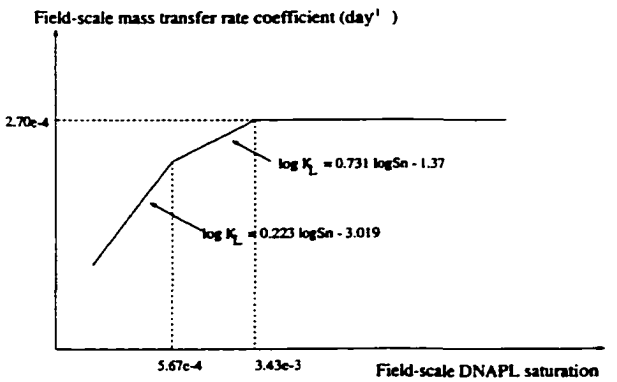

Figure 5.2: Field-scale mass transfer rate coefficient of 1,1,1-TCA for a velocity of 0.01 $m \cdot day^{-1}$

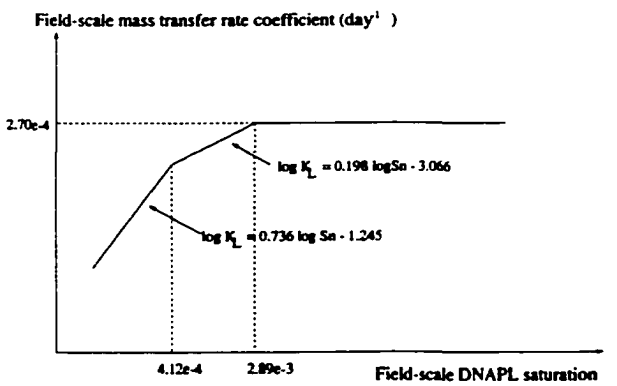

Figure 5.3: Field-scale mass transfer rate coefficient of 1,1,2-TCA and chloroform for a velocity of 0.01 $m \cdot day^{-1}$

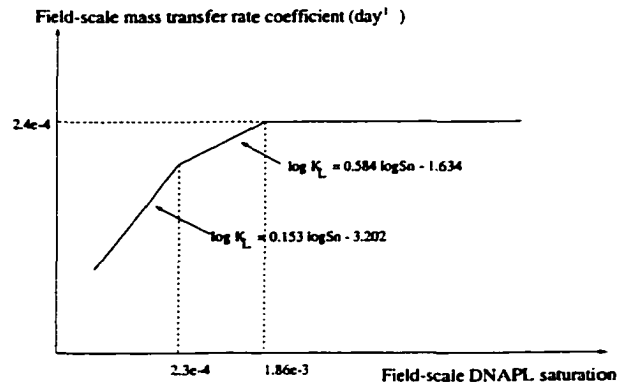

Figure 5.4: Field-scale mass transfer rate coefficient of 1,1,1-TCA for a velocity of 0.1 m·day^{-1}

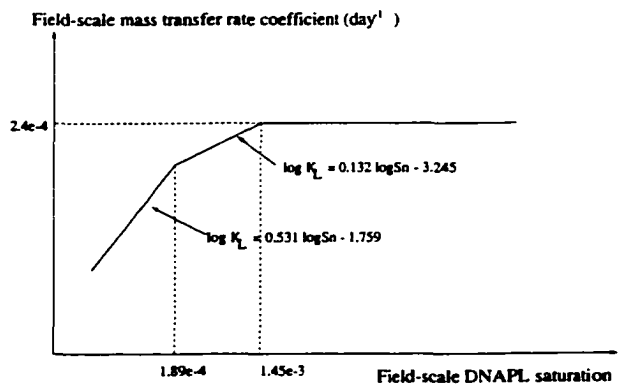

Figure 5.5: Field-scale mass transfer rate coefficient of 1,1,2-TCA and chloroform for a velocity of 0.1 m·day^{-1}

5.1 One component DNAPL case

In this section, a DNAPL source zone containing a single-component DNAPL will be studied. Three different DNAPLs with different solubilities are considered. These are 1,1,1-trichloroethane or methyl chloroform (1,1,1-TCA) , 1,1,2-trichloroethane or vinyl trichloroform (1,1,2-TCA) and chloroform. The chemical properties of these DNAPLs are shown in table(5.1) [21]. Each DNAPL will be in the seepage velocity of 0.1 and 0.01 m·day^{-1}. There will then be six scenarios in this section.

Chemical properties	1,1,1-TCA	1,1,2-TCA	chloroform
Chemical formula	$C_2H_3Cl_3$	$C_2H_3Cl_3$	$CHCl_3$
Solubility limit (kg·m^{-3})	1.5	4.5	8.2
Density (kg·m^{-3})	1339.0	1439.0	1483.2
Half life (year)	0.5	139.2	1.25
Molecular weight (g·mole^{-1})	133.4	133.4	119.38
K_{oc} (cm^3·g^{-1})	152.0	56.0	47.0

Table 5.1: Chemical properties of DNAPLs

The mass transfer rate was calculated at the beginning of each time step using the eqn.(3.16). The concentration at the center of the source zone then was estimated using eqn.(3.17). The remaining DNAPL mass was estimated by subtracting the initial mass by the amount of mass being transfered from the source zone during that time step.

Results are shown in the figures (5.6), (5.7), (5.8), (5.9), (5.10), and (5.11) Figures (5.6), (5.7), (5.8), (5.9), (5.10), and (5.11) compare the concentration, the remaining mass and the mass transfer rate between 1,1,1-TCA, 1,1,2-TCA and chloroform in velocities of 0.1 and 0.01 m·day^{-1}.

Concentrations and mass transfer rates of all three DNAPLs behave in a similar pattern. The concentration is initially equal to zero because the groundwater flow

into a DNAPL subzone is free from the contaminant. Then the concentration starts to increase rapidly because the mass transfer rate at early time is also very high due to the highest concentration difference between the solubility and the aqueous-phase concentration which is initially zero. The high mass transfer rate causes the increase in the concentration. However, the mass transfer rate decreases rapidly and stays constant since the concentration difference between the solubility and the aqueous-phase concentration is now very small. The constant mass transfer rate causes the concentration to be constant. At later time when the mass is almost depleted, the mass transfer rate starts to decrease. This is because the mass transfer rate coefficient is now a function of the DNAPL saturation. The decrease mass transfer rate also causes the decrease in the concentration. When the mass is depleted, the concentration still persists in the subzone. It takes some time to the aqueous-phase concentration to be carried away by the transport process. During this time, the concentration keeps decreasing until it equals zero. The mass transfer rate of each component at two velocities are nearly the same because the mass transfer rate coefficient at the two velocities are almost equal at early time.

The results for concentration, mass transfer rate and remaining mass are similar for all three DNAPLs. The concentration at a velocity of 0.01 m·day^{-1} are higher and stay longer in the system than the concentration at a velocity of 0.1 m·day^{-1}. The lower seepage velocity remove the dissolved mass from the source zone slower than the higher seepage velocity. The aqueous phase mass persists in the source zone longer. And concentrations estimated at the center of the source zone are far lower than its solubility. This causes by the very small field-scale mass transfer rate coefficient which gives the rate-limited mass transfer rate resulting in the small concentration.

The mass transfer rates at two velocities studied are rather constant. This constant

mass transfer rate is caused by the constant mass transfer rate coefficient when the DNAPL saturation is still high. However, when the DNAPL saturation is very low, the mass transfer rate coefficient decreases as a function of the DNAPL saturation. Consequently, the mass transfer rate decreases.

Table (5.2) shows the mass depletion time and the concentration depletion time of three component DNAPLs in both velocities. The difference in the mass depletion time in both seepage velocities in the DNAPL with the relatively high solubility is very small, about a year difference between both velocities. There exists differences in depletion time for two velocities studied in the DNAPL with the relatively low solubility. The difference in the mass depletion time of 1,1,1-TCA between two velocities is about 5 years. This may suggest that in a single component DNAPL with relatively high solubility, the seepage velocity has less effect on the dissolution process than its solubility. Table (5.2) also shows that the concentration depletion time is larger than the mass depletion time in all three DNAPL and in both velocities. Even though the DNAPL mass is depleted, the aqueous-phase concentration still persists in the system. The advective-dispersive transport then carries the concentration away from a source zone.

Figures(5.7) and (5.10) show that the higher the solubility is, the faster the mass depletion time will be in both velocities. Figures(5.6), (5.8), (5.9), and (5.11) show that the highest soluble component give the highest concentration and the highest mass transfer rate.

Component	Mass depletion time (year)		Concentration depletion time (year)	
	v=0.01 m·day^{-1}	v=0.1 m·day^{-1}	v=0.01 m·day^{-1}	v=0.1 m·day^{-1}
1,1,1-TCA	109	104	115	105
1,1,2-TCA	35	34	41	35
chloroform	20	19	25	20

Table 5.2: Mass depletion time and concentration depletion time

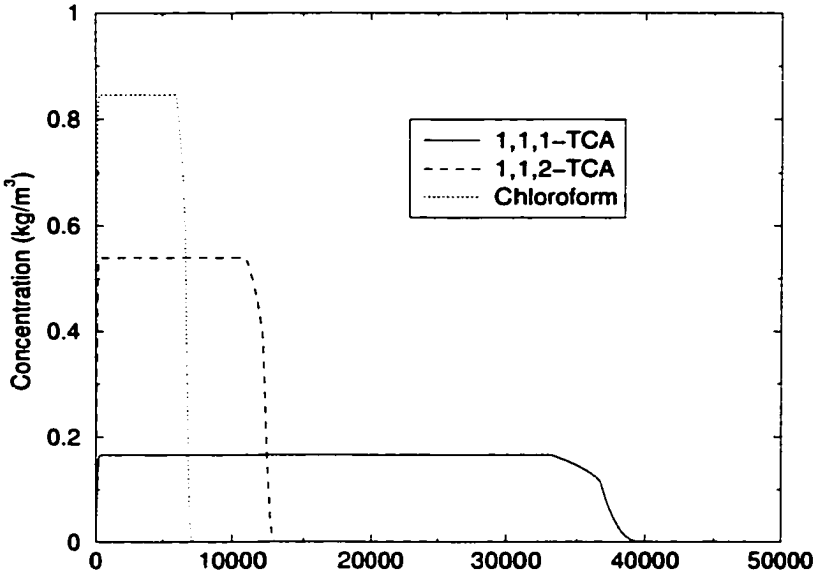

Figure 5.6: Concentration for v = 0.01 m/day

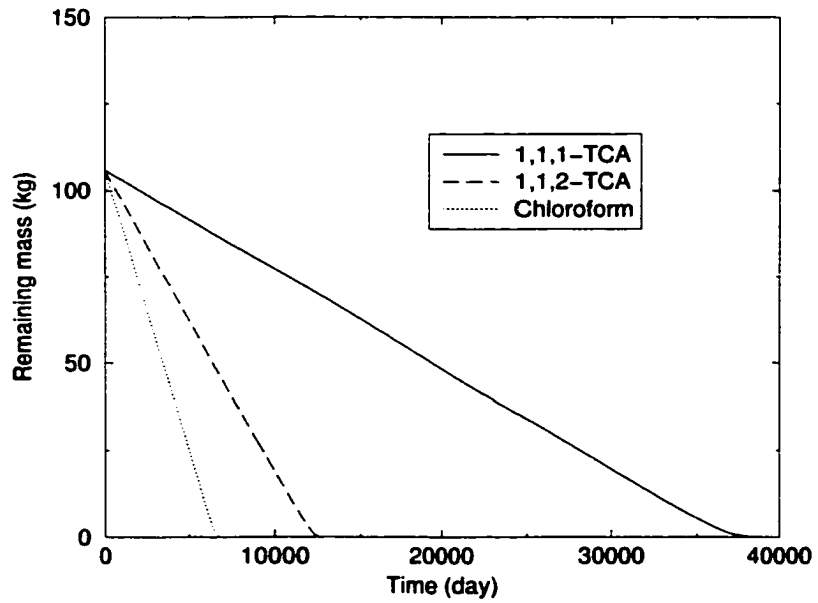

Figure 5.7: Remaining mass for v = 0.01 m/day

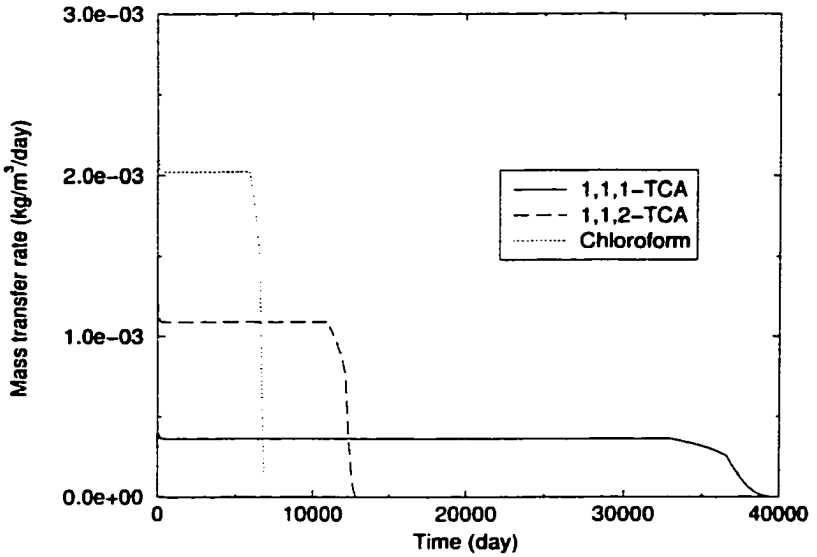

Figure 5.8: Mass transfer rate for v = 0.01 m/day

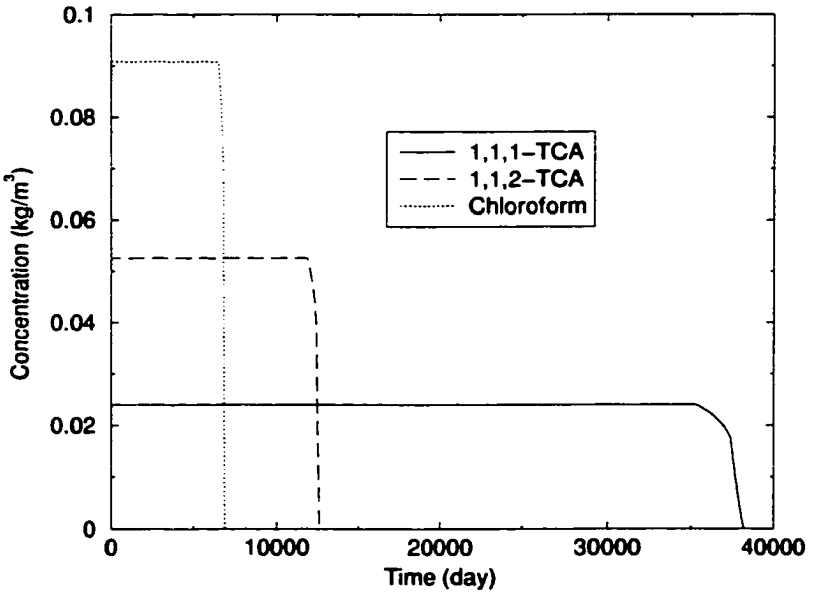

Figure 5.9: Concentration for v = 0.1 m/day

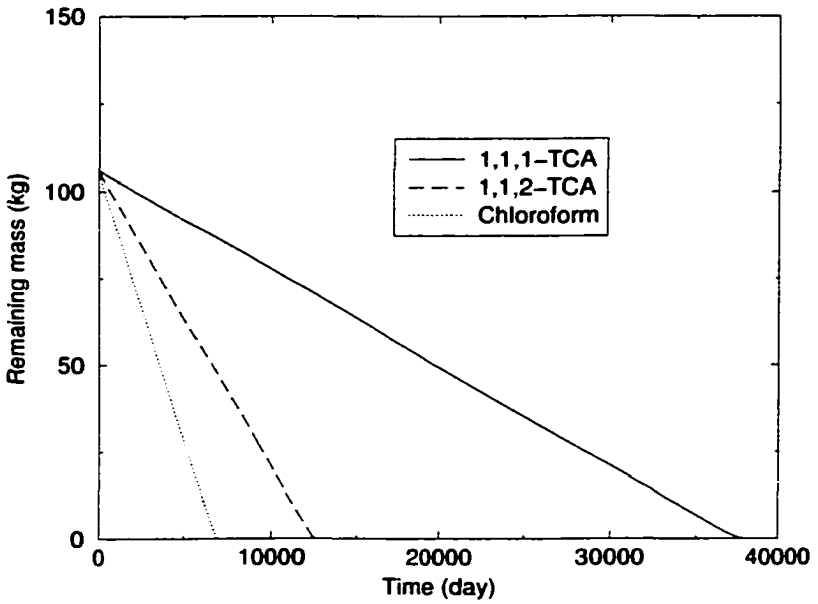

Figure 5.10: Remaining mass for v = 0.1 m/day

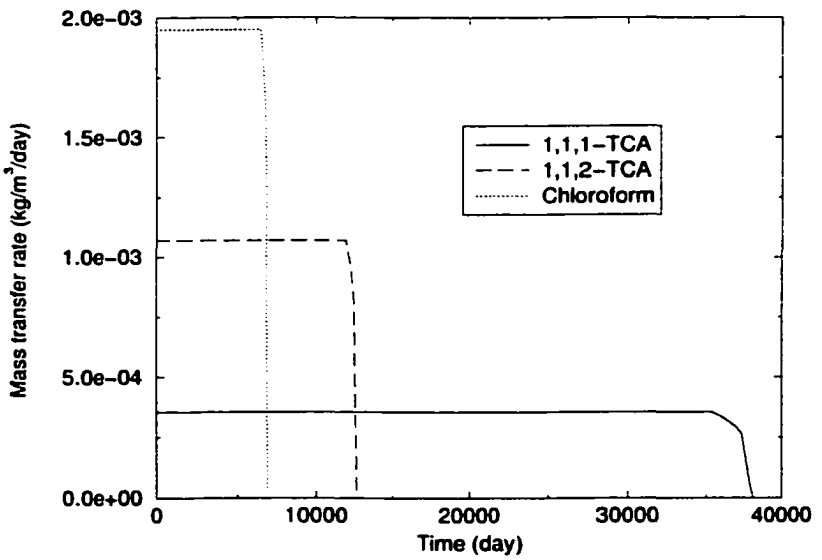

Figure 5.11: Mass transfer rate for v = 0.1 m/day

5.2 Multiple-component case

5.2.1 A two-component mixture

In most of the contaminant cases in the groundwater, there are mixtures of DNAPLs. Therefore, the dissolution of the two components DNAPLs will be studied. There are three cases or combinations of DNAPLs used in this case. These are the mixture of 1,1,1-TCA with 1,1,2-TCA, the mixture of 1,1,1-TCA with chloroform and the mixture of 1,1,2-TCA with chloroform. The differences in the solubilities will show the effect of one DNAPL onto the other when there are mixtures of DNAPL in the groundwater such as how the less soluble component would behave with the presence of the more soluble component in the groundwater.

The case studies assume both DNAPLs have the same initial mass. The program runs until both masses are depleted from the source zone. The amount of mass in this two components DNAPLs case will be the same as the single DNAPL case thus results can be compared to determine if the presence of another DNAPL has any effect on the depletion time or the concentration.

The effective solubility of each component will be calcuated using eqn.(2.19). The mass transfer rate of each component will be estimated using eqn.(3.20) and the concentration at the center of the source zone can be estimated using eqn.(3.21).

Figures(5.12), (5.14), (5.16) and (5.18) are the concentration vs. time, the remaining mass vs. time, the mass transfer rate vs. time and the mole fraction vs. time of the mixture of 1,1,1-TCA and chloroform at a velocity of 0.01 m·day^{-1}. Figures(5.13), (5.15), (5.17) and (5.19) are the concentration vs. time, the remaining mass vs. time, the mass transfer rate vs. time and the mole fraction vs. time of the mixture of 1,1,1-TCA and chloroform at a velocity of 0.1 m·day^{-1}. Figures(5.20), (5.22), (5.24) and (5.26) are the concentration vs. time, the remaining mass vs. time, the mass

transfer rate vs. time and the mole fraction vs. time of the mixture of 1,1,2-TCA and chloroform at a velocity of 0.01 m·day^{-1}. Figures(5.21), (5.23), (5.25) and (5.27) are the concentration vs. time, the remaining mass vs. time, the mass transfer rate vs. time and the mole fraction vs. time of the mixture of 1,1,2-TCA and chloroform at a velocity of 0.1 m·day^{-1}. Figures(5.28), (5.30), (5.32) and (5.34) are the concentration vs. time, the remaining mass vs. time, the mass transfer rate vs. time and the mole fraction vs. time of the mixture of 1,1,1-TCA and 1,1,2-TCA at a velocity of 0.01 m·day^{-1}. Figures(5.29), (5.31), (5.33) and (5.35) are the concentration vs. time, the remaining mass vs. time, the mass transfer rate vs. time and the mole fraction vs. time of the mixture of 1,1,1-TCA and 1,1,2-TCA at a velocity of 0.1 m·day^{-1}.

There are some similar results to the single-component case shown in this case. For example, concentrations in a velocity of 0.01 m·day^{-1} are higher than concentrations in a velocity of 0.1 m·day^{-1}. For the mixture of two components case, concentrations of the more soluble component are higher at early time and then rapidly decrease. Concentrations of the less soluble component gradually increase (figures(5.12), (5.13), (5.20), (5.21), (5.28) and (5.29)).

The mass transfer rate of the more soluble component are relatively high at early time and rapidly decrease while the mass transfer rate of the less soluble component is gradually increasing. It has the same pattern as the concentration (figures(5.16), (5.17), (5.24), (5.25), (5.32) and (5.33)). In all cases, the mixtures have the same mole fraction therefore the higher solubility component will then have the higher effective solubility in which resulting in the higher mass transfer rate at early time.

The mole fraction of the more soluble component decreases while the mole fraction of the less soluble component increases (figures(5.18), (5.19), (5.26), (5.27), (5.34) and (5.35)). The decrease in rates of the mole fraction in the mixture of 1,1,1-TCA with

chloroform is the highest comparing with the mixture of 1,1,2-TCA with chloroform and the mixture of 1,1,1-TCA with 1,1,2-TCA. This is because the difference between 1,1,1-TCA solubility and chloroform solubility are the highest.

The masses of the more soluble component decrease faster at early time than the less soluble component (figures(5.14), (5.15), (5.22), (5.23), (5.30) and (5.31)). The rate of decreasing mass of the more soluble component will decline at later time. This declination of the decreasing mass is also shown the same behavior in the mole fraction.

Table (5.3) shows the mass depletion time and the concentration time of each component in the two components DNAPLs system in both velocities. The results shows that the mass depletion time of each component in a multi-component DNAPLs is about the same. The mole fraction controls the mass transfer rate. The mole fraction of the more soluble component decreases rapidly and the mole fraction of the less soluble component increases at early time. The mole fraction of the more soluble component is very small compared to the mole fraction of the less soluble at later time. This small mole fraction causes the small effective solubility resulting in small mass transfer rate at later time. However, even though the less soluble component has the large mole fraction, its solubility is small. This combination causes still a small mass transfer rate. This process causes the mass depletion time of all component in a multi-component DNAPLs regardless of its solubility to be approximately the same.

The concentration depletion time of each component in a multi-component DNAPLs is longer than the mass depletion time. This is a similar results as in a single component DNAPL. Comparing the concentration depletion time between two velocities of the same component, the concentration depletion time in the lower velocity takes longer to deplete. The process that moves the concentration away from a source zone

is the transport process so the lower velocity takes longer for the concentration to deplete. When compare the concentration depletion time between each component in a multi-component DNAPLs system in the same velocity, the results showed that the less soluble component takes longer for the concentration to deplete. Even though the transport process controls the depletion of the concentration, the remaining concentration of the less soluble component is higher than the concentration of the more soluble component, therefore it takes longer for the concentration to deplete.

Component	Mass depletion time (year)		Concentration depletion time	
	v=0.01 m·day^{-1}	v=0.1 m·day^{-1}	v=0.01 m·day^{-1}	v=0.1 m·d
1,1,1-TCA and chloroform				
1,1,1-TCA	128	123	136	124
chloroform	128	123	133	124
1,1,2-TCA and chloroform				
1,1,2-TCA	54	53	61	54
chloroform	54	53	60	54
1,1,1-TCA and 1,1,2-TCA				
1,1,1-TCA	144	139	153	140
1,1,2-TCA	144	139	150	139

Table 5.3: Mass depletion time and concentration depletion time

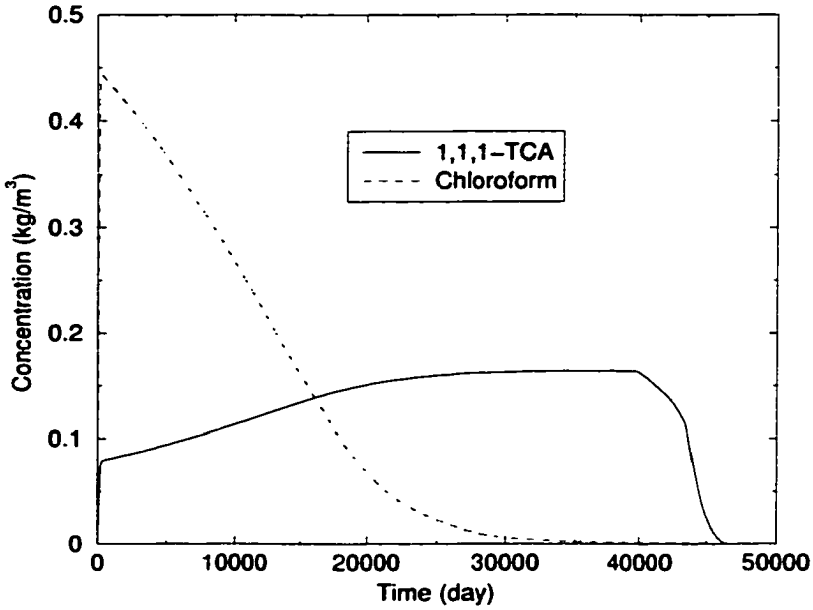

Figure 5.12: Concentration for v = 0.01 m/day

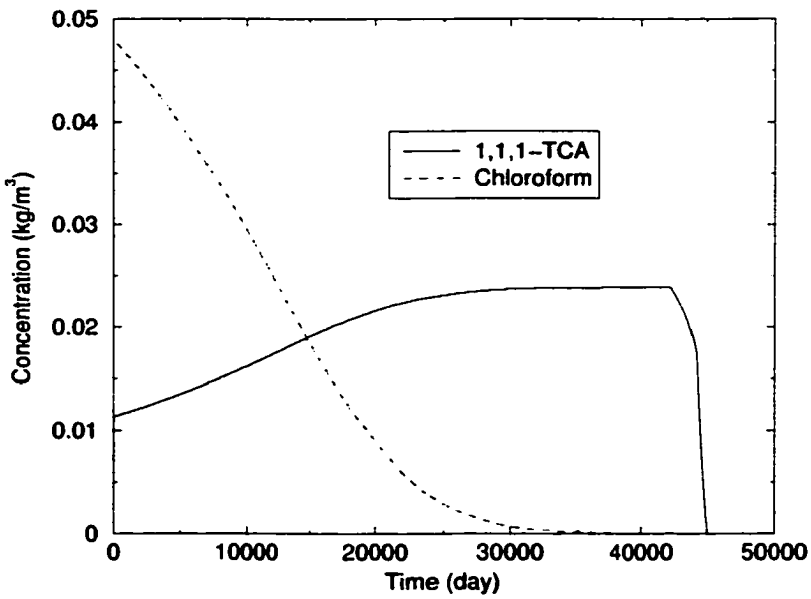

Figure 5.13: Concentration for v = 0.1 m/day

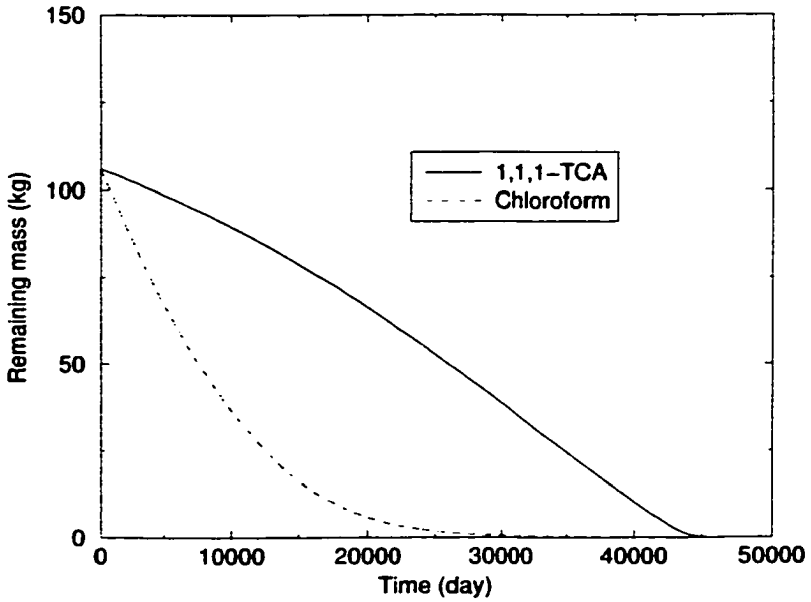

Figure 5.14: Remaining mass for v = 0.01 m/day

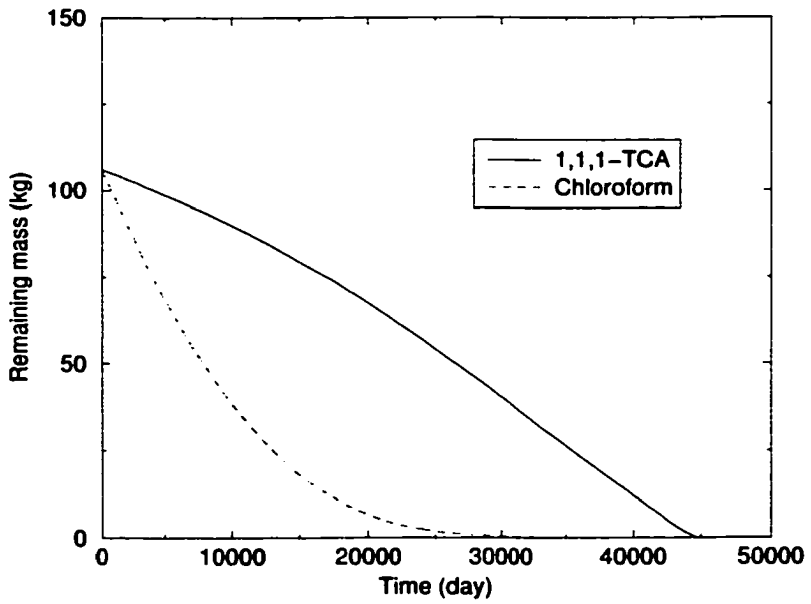

Figure 5.15: Remaining mass for v = 0.1 m/day

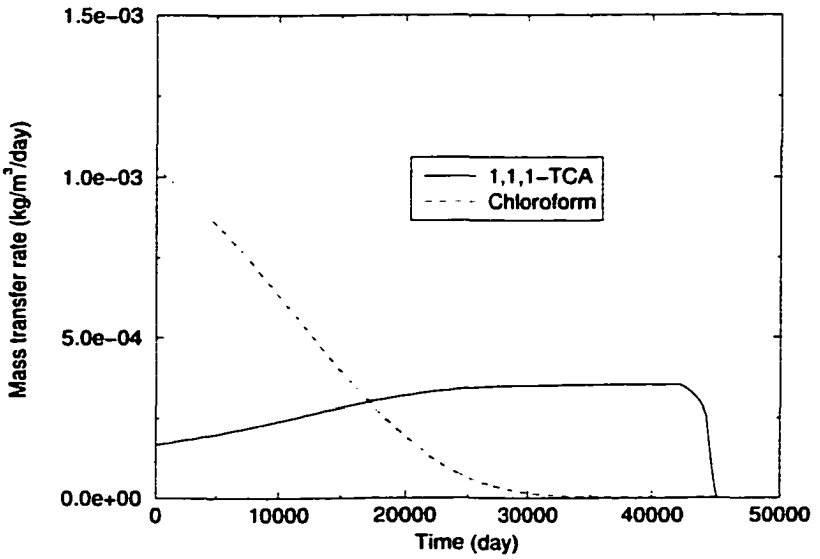

Figure 5.16: Mass transfer rate for v = 0.01 m/day

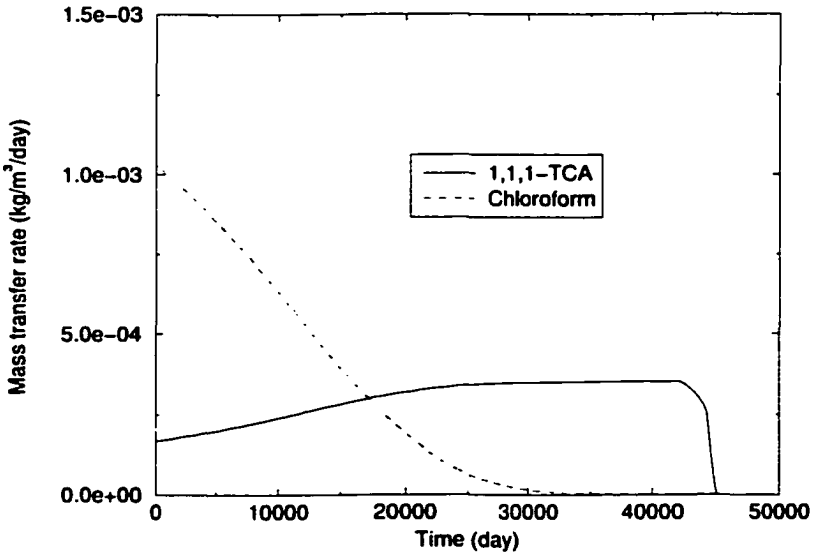

Figure 5.17: Mass transfer rate for v = 0.1 m/day

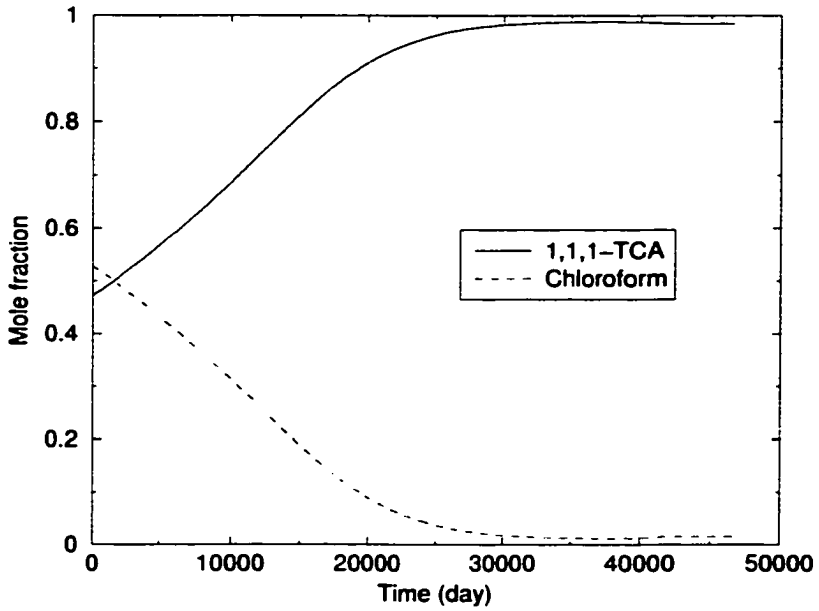

Figure 5.18: Mole fraction for v = 0.01 m/day

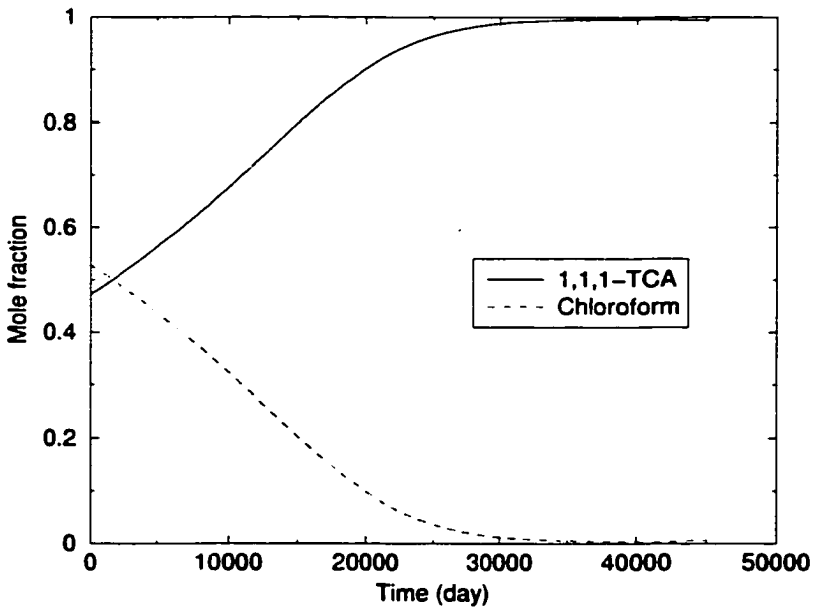

Figure 5.19: Mole fraction for v = 0.1 m/day

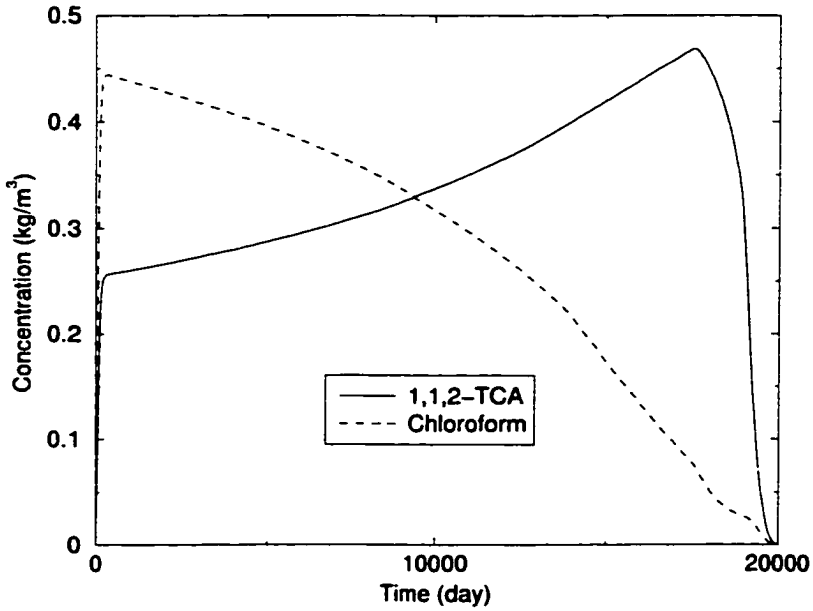

Figure 5.20: Concentration for v = 0.01 m/day

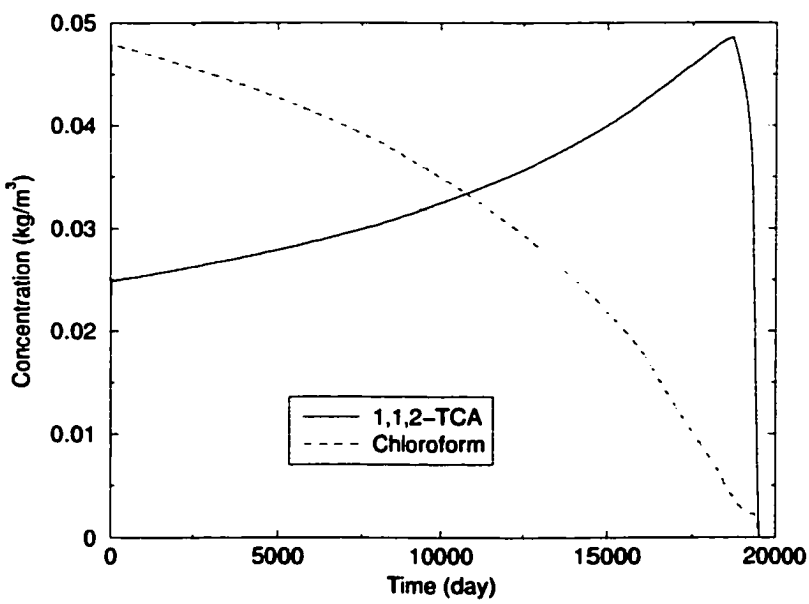

Figure 5.21: Concentration for v = 0.1 m/day

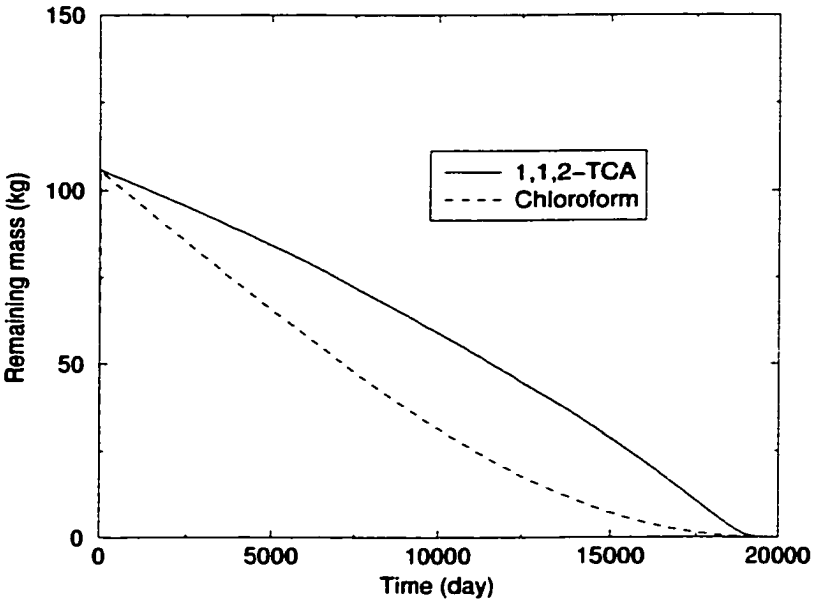

Figure 5.22: Remaining mass for v = 0.01 m/day

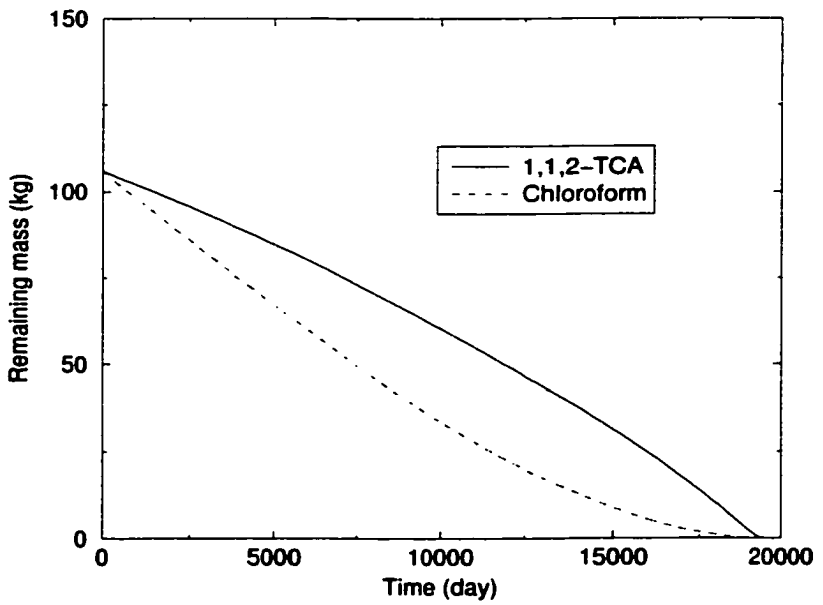

Figure 5.23: Remaining mass for v = 0.1 m/day

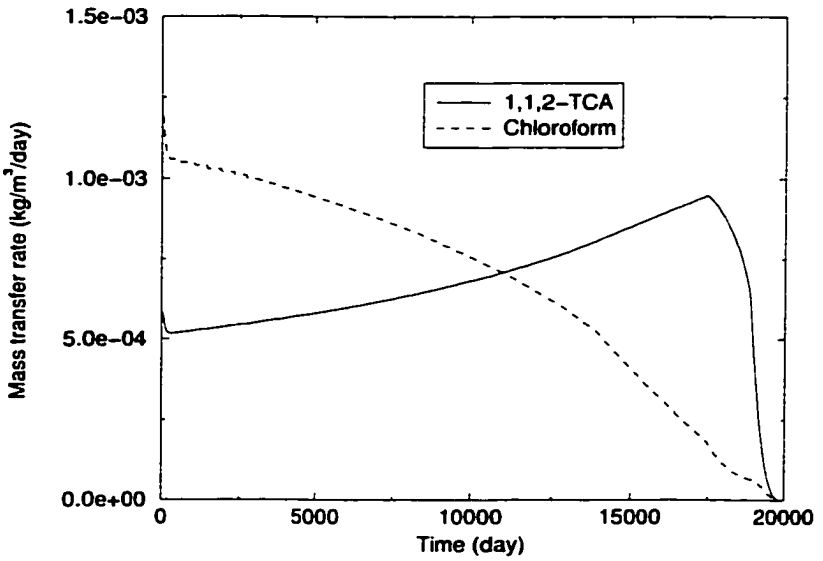

Figure 5.24: Mass transfer rate for v = 0.01 m/day

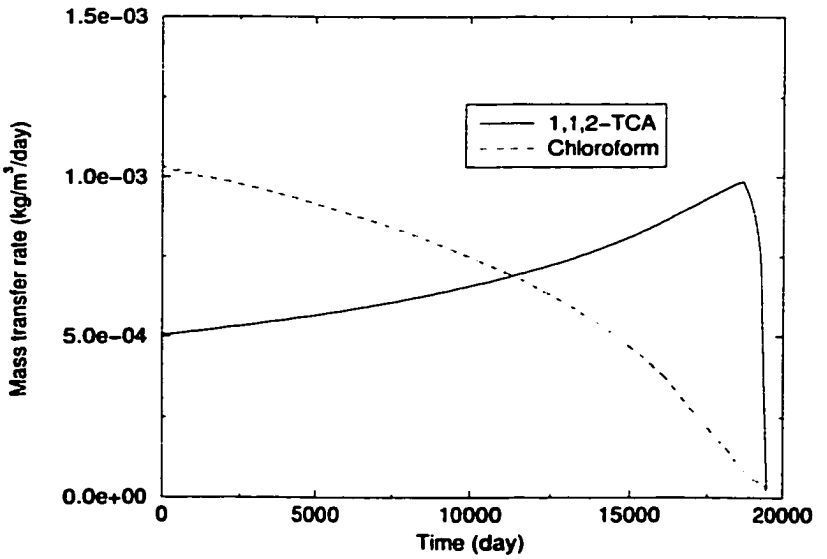

Figure 5.25: Mass transfer rate for v = 0.1 m/day

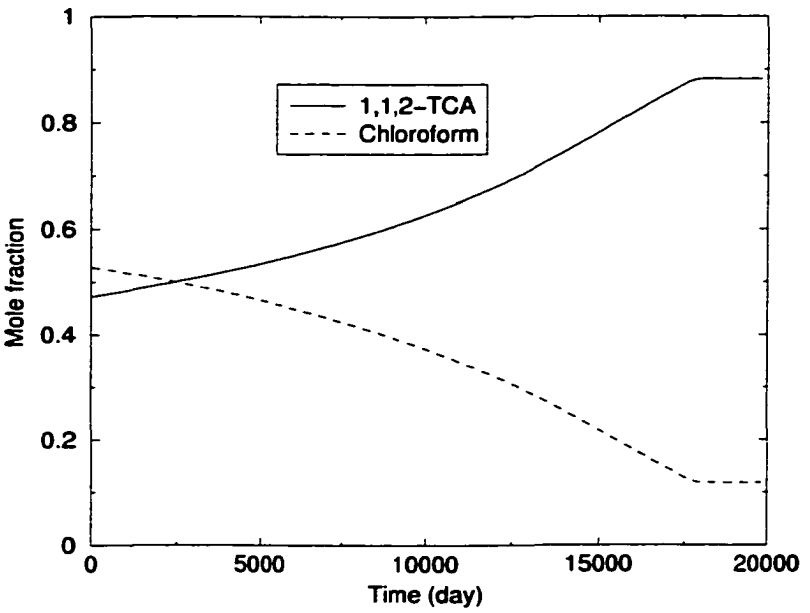

Figure 5.26: Mole fraction for v = 0.01 m/day

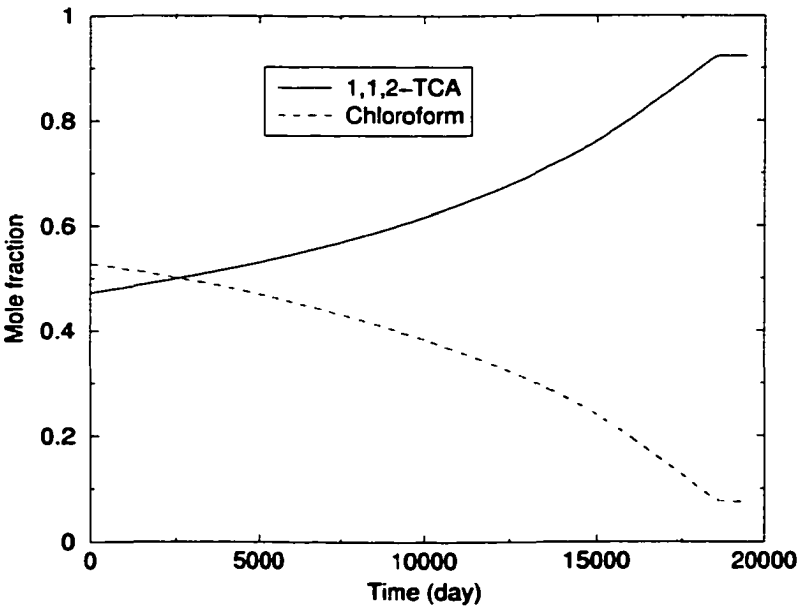

Figure 5.27: Mole fraction for v = 0.1 m/day

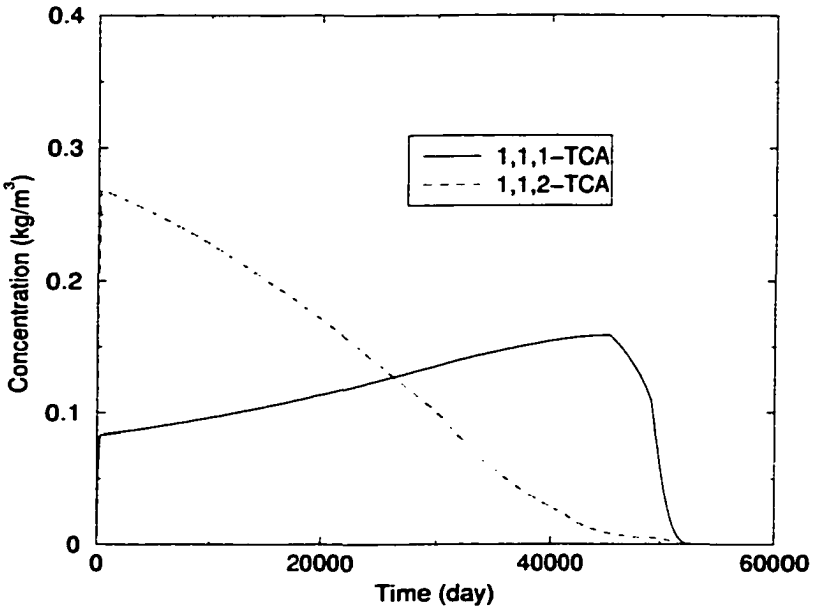

Figure 5.28: Concentration for v = 0.01 m/day

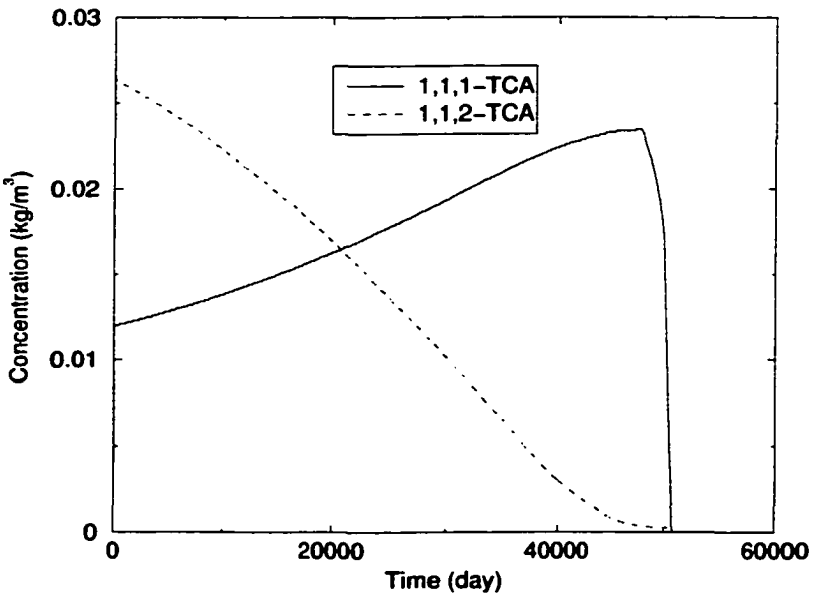

Figure 5.29: Concentration for v = 0.1 m/day

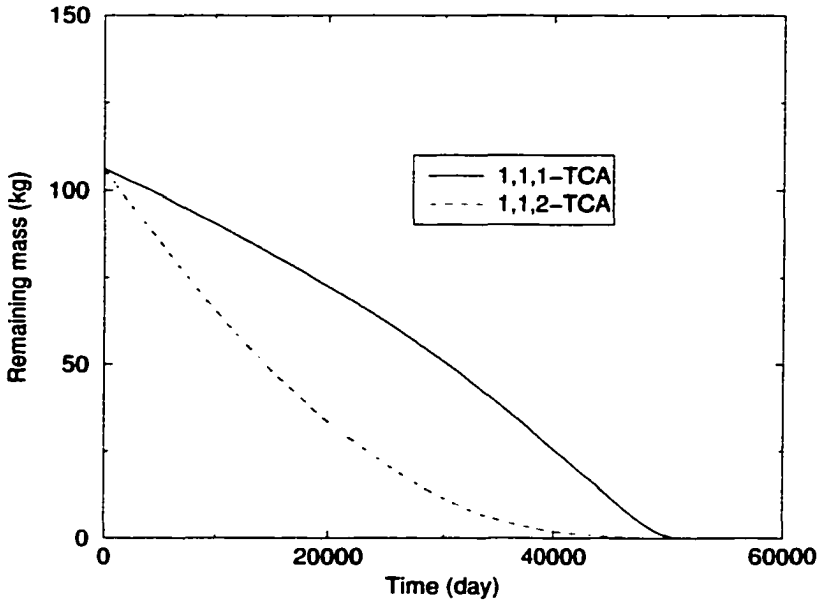

Figure 5.30: Remaining mass for v = 0.01 m/day

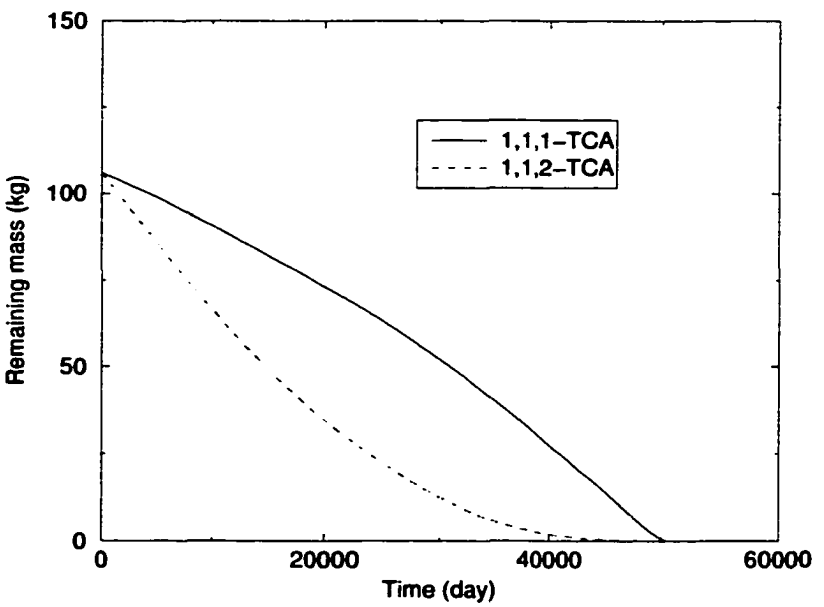

Figure 5.31: Remaining mass for v = 0.1 m/day

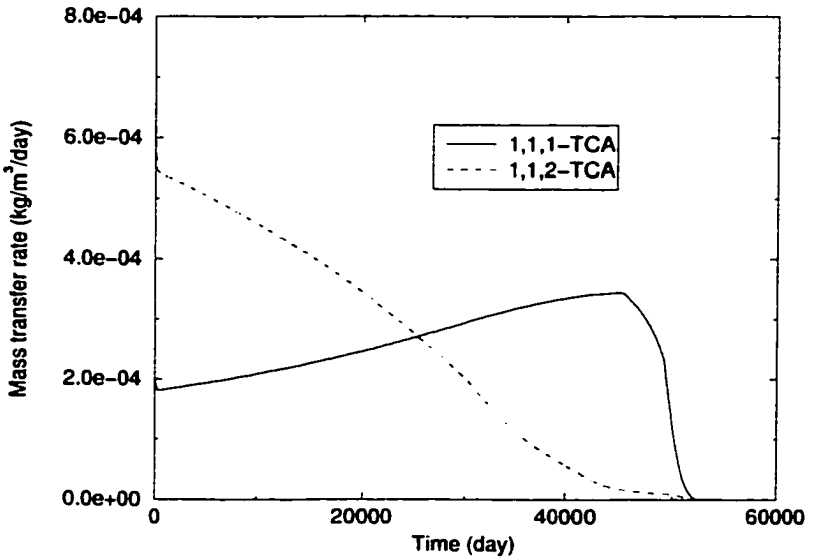

Figure 5.32: Mass transfer rate for v = 0.01 m/day

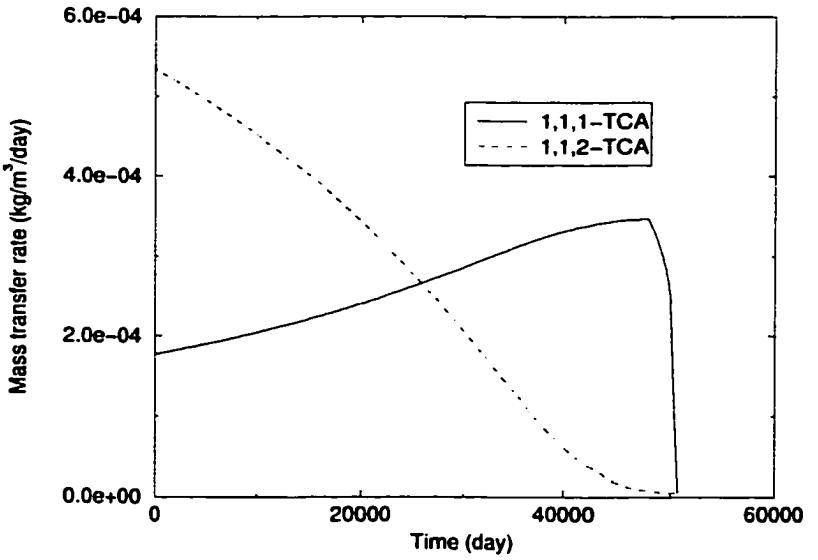

Figure 5.33: Mass transfer rate for v = 0.1 m/day

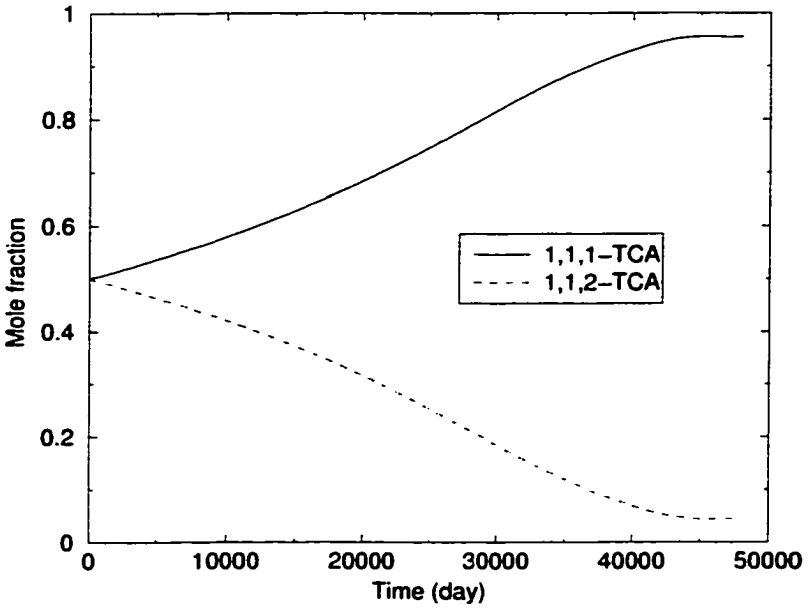

Figure 5.34: Mole fraction for v = 0.01 m/day

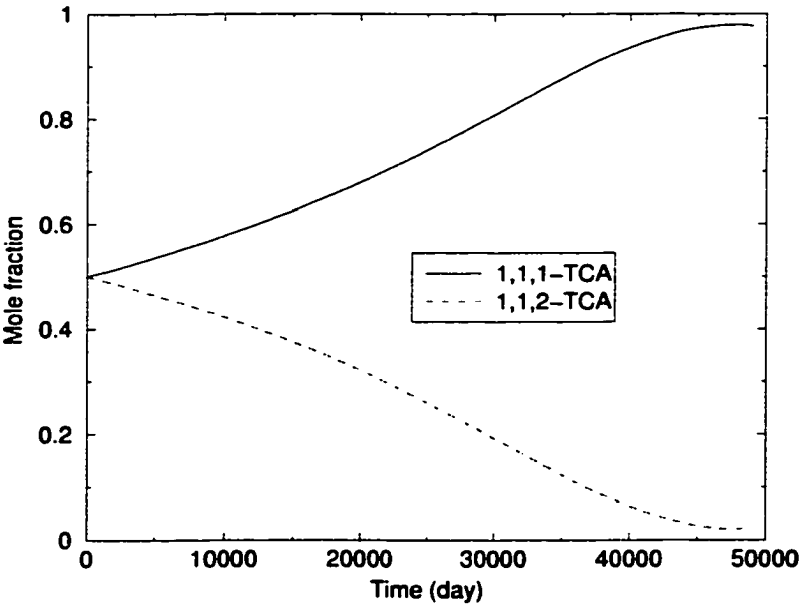

Figure 5.35: Mole fraction for v = 0.1 m/day

5.2.2 A three-component mixture

Chloroform, 1,1,1-TCA and 1,1,2-TCA will be in a source zone. Initial mass of all components will be the same which contributing to the mole fraction of 0.32, 0.32 and 0.36 for 1,1,1-TCA, 1,1,2-TCA and chloroform, respectively. Program runs until the mass is depleted.

Figures (5.36), (5.38), (5.40) and (5.42) show the concentration vs. time, the remaining mass vs. time, the mass transfer rate vs. time and the mole fraction vs. time for a velocity of 0.01 m·day^{-1}. Figures (5.37), (5.39), (5.41) and (5.43) show the concentration vs. time, the remaining mass vs. time, the mass transfer rate vs. time and the mole fraction vs. time for a velocity of 0.1 m·day^{-1}.

There are some similar results in this case to the single-component and the two DNAPLs components case. Concentrations in a velocity of 0.01 m·day^{-1} are higher than concentrations in a velocity of 0.1 m·day^{-1}. The mass depletion time in the lower velocity is longer than the mass depletion time in the higher velocity.

In the mixture of three DNAPLs, at early time mass transfer rates of chloroform decrease rapidly while mass transfer rates of 1,1,1-TCA gradually increase. Mass transfer rate of 1,1,2-TCA are rather constant at early time (figures(5.40), and (5.41)). Concentrations of chloroform, 1,1,1-TCA and 1,1,2-TCA follow the same pattern as its mass transfer rate (figures(5.36), and (5.37)). Masses of chloroform and 1,1,2-TCA decreases rapidly at early time and gradually decreases at later time. On the opposite, masses of 1,1,1-TCA gradually decreases at early time but rapidly decreasing at later time (figures(5.38), and (5.39)). At early time, the mole fraction of chloroform decreases rapidly. The mole fraction of 1,1,1-TCA increases while the mole fraction of 1,1,2-TCA gradually decreases (figures(5.42), and (5.43)). When the mole fraction of chloroform is relatively small, the mole fraction of 1,1,2-TCA starts to decrease

rapidly.

In this system, the dissolution of the component with the highest solubility (chloroform) and the lowest solubility (1,1,1-TCA) will be very active at early time. And when the mass of the component with the highest solubility is relatively small, then the component with the second highest solubility will start to be active in its dissolution process.

Table (5.4) shows the mass depletion time and the concentration depletion time of each component in the three components DNAPLs case. The results are similar to the two components DNAPLs case that the mass depletion time of each component is approximately the same. The concentration takes longer to deplete. Comparing the mass depletion time and the concentration depletion time between two velocities, the lower velocity takes longer for both mass and concentration to deplete.

Component in the mixture	Mass depletion time (year)		Concentration depletion time	
	v=0.01 m·day^{-1}	v=0.1 m·day^{-1}	v=0.01 m·day^{-1}	v=0.1 m·
1,1,1-TCA	163	158	172	159
1,1,2-TCA	163	158	169	158
chloroform	163	158	169	158

Table 5.4: Mass depletion time and concentration depletion time

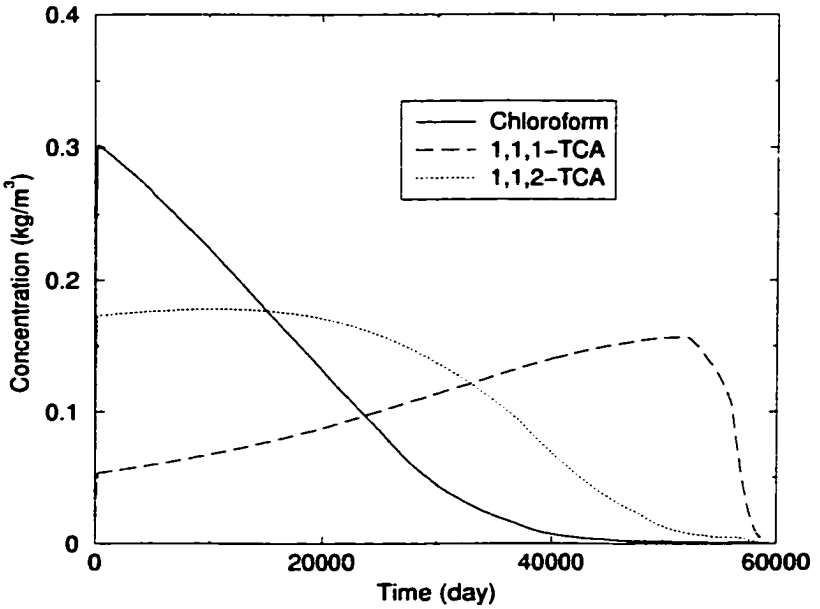

Figure 5.36: Concentration for v = 0.01 m/day

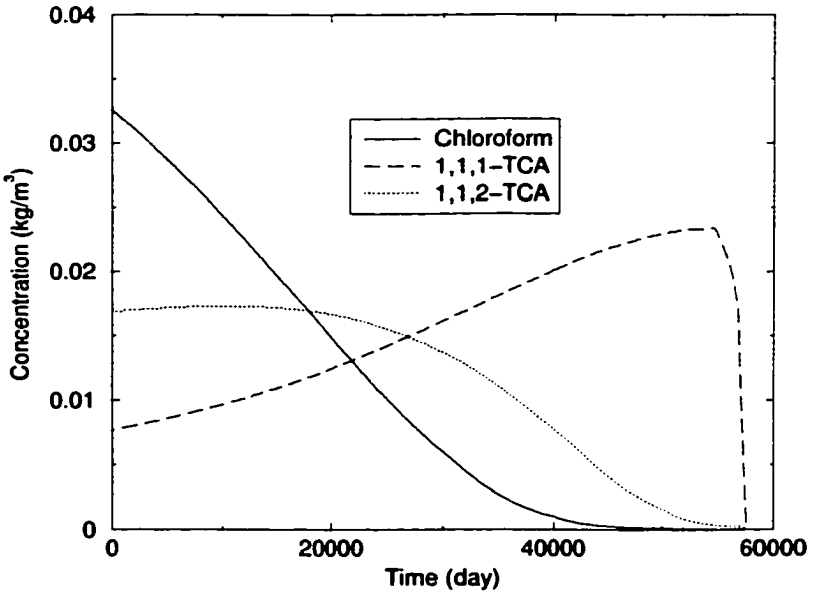

Figure 5.37: Concentration for v = 0.1 m/day

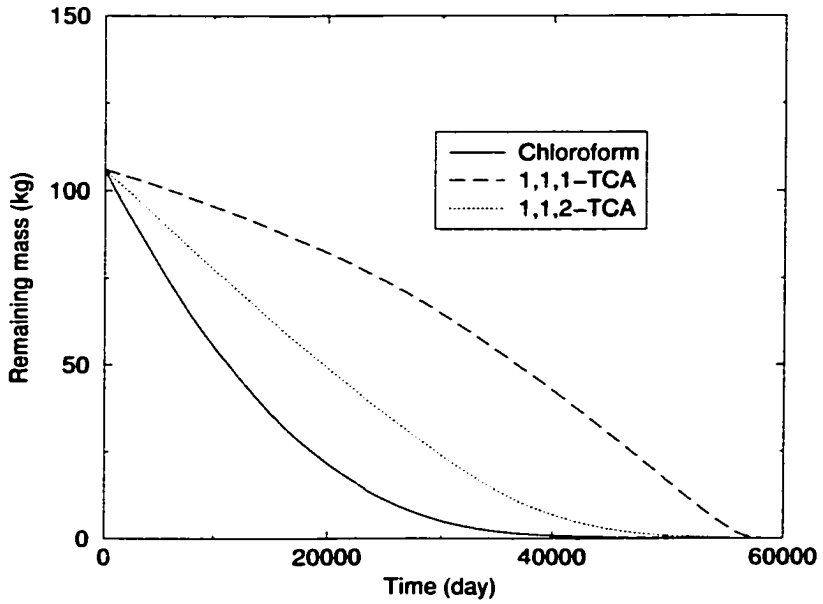

Figure 5.38: Remaining mass for v = 0.01 m/day

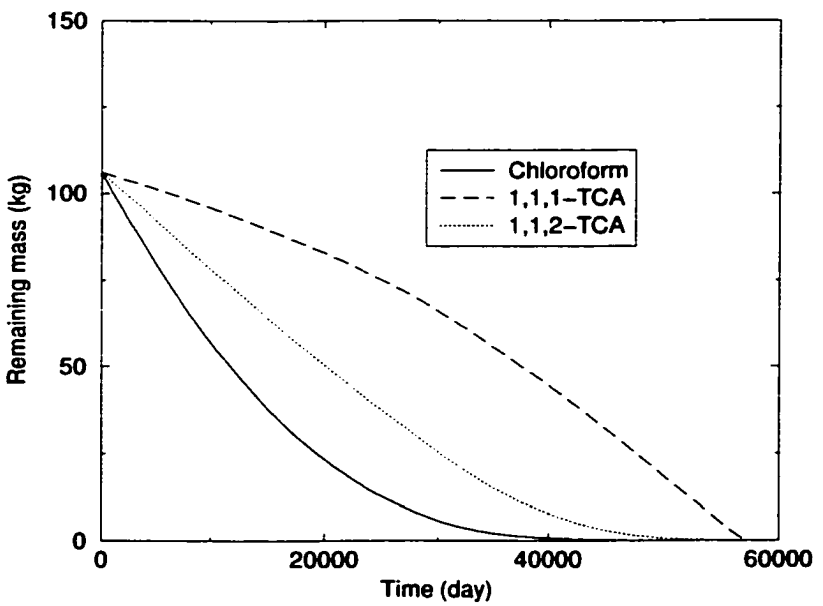

Figure 5.39: Remaining mass for v = 0.1 m/day

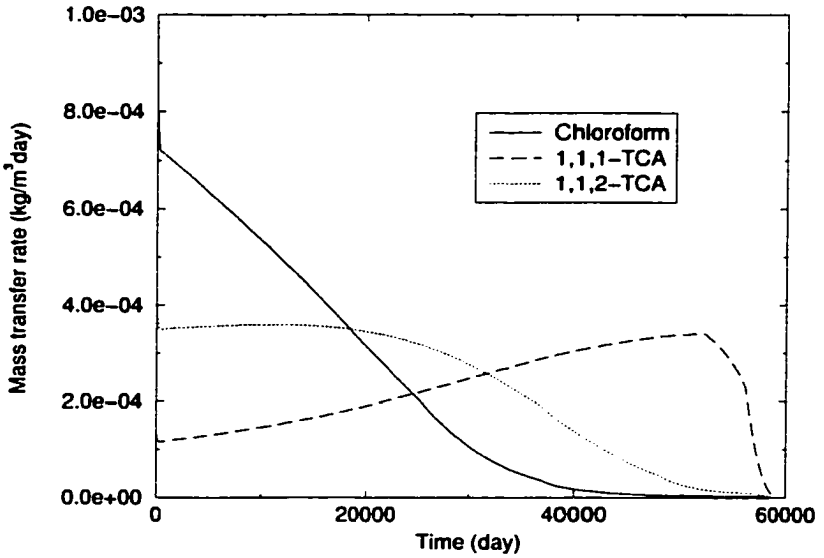

Figure 5.40: Mass transfer rate for v = 0.01 m/day

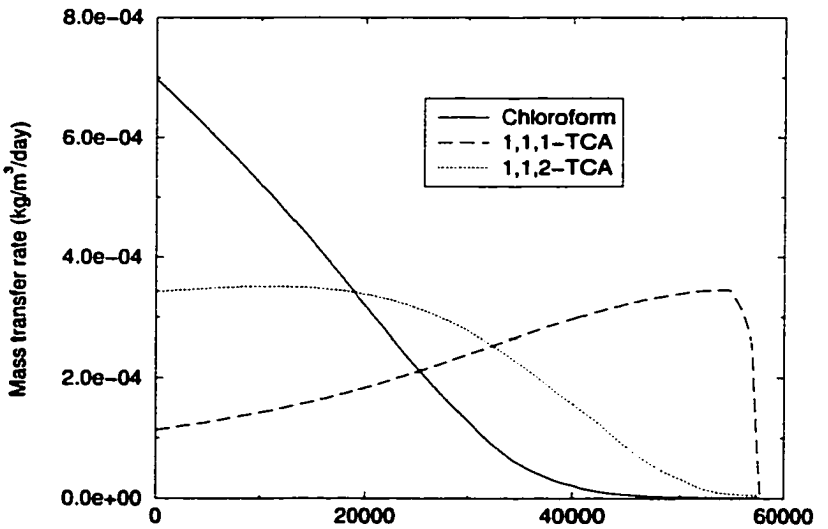

Figure 5.41: Mass transfer rate for v = 0.1 m/day

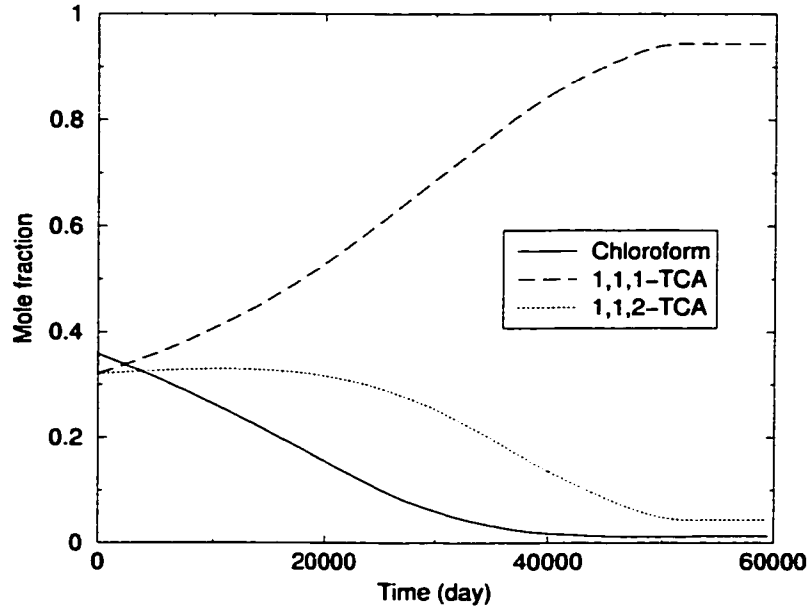

Figure 5.42: Mole fraction for v = 0.01 m/day

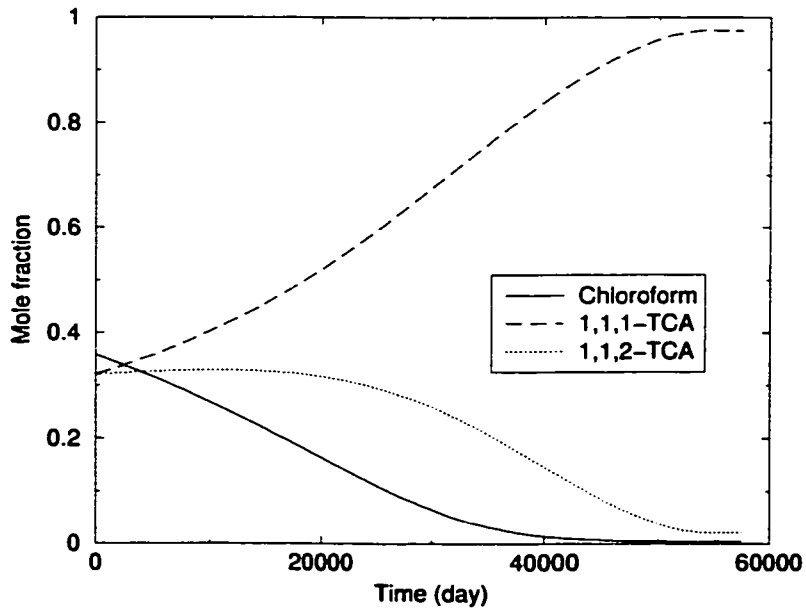

Figure 5.43: Mole fraction for v = 0.1 m/day

5.3 The effect of component mixtures on the mass transfer rate

The comparison of the mass depletion time of chloroform, 1,1,1-TCA and 1,1,2-TCA between a single-component and multicomponent case will be made. Figures (5.44), and (5.45) show the remaining mass vs. time of chloroform in a single component and in a multicomponent cases at velocities of 0.01 and 0.1 m·day^{-1}. Figures (5.46), and (5.47) show the remaining mass vs. time of 1,1,1-TCA in a single component and in a multicomponent cases at velocities of 0.01 and 0.1 m·day^{-1}. Figures (5.48), and (5.49) show the remaining mass vs. time of 1,1,2-TCA in a single component and in a multicomponent cases at velocities of 0.01 and 0.1 m·day^{-1}.

Cases	v=0.01 m·day^{-1}	v=0.1 m·day^{-1}
Single-component		
chloroform	20	19
1,1,1-TCA	109	104
1,1,2-TCA	35	34
Multi-component		
1,1,1-TCA+chloroform	128	123
1,1,2-TCA+chloroform	54	53
1,1,1-TCA+1,1,2-TCA	144	139
1,1,1-TCA+1,1,2-TCA+chloroform	163	158

Table 5.5: The mass depletion time of single-component and multi-component cases

Table (5.5) shows the mass depletion time of chloroform, 1,1,1-TCA and 1,1,2-TCA in a single component and multicomponent systems. It obviously shows that the mass depletion time increases dramatically in a multicomponent system. The mole fraction and effective solubility of each component in a multi-component DNAPL cause the longer mass depletion time than a single component DNAPL. The combination of the mixture also has the effect on the mass depletion time. For example, at a seepage velocity of 0.01 m·day^{-1} when chloroform is mixed with 1,1,2-TCA the mass

depletion time is 53 years. However at the same velocity, the mass depletion time of the mixture of chloroform and 1,1,1-TCA has increased to 128 years. Similarly, for the mixture of 1,1,2-TCA when it is mixed with 1,1,1-TCA the mass depletion time is 144 years at a velocity of 0.01 $m \cdot day^{-1}$. The mixture of relatively high solubility such as the mixture of 1,1,2-TCA and chloroform have relatively high effective solubility, therefore relatively high mass transfer rate. In the mixture of relatively high and low solubility such as the mixture of chloroform and 1,1,1-TCA, even though the mole fraction of 1,1,1-TCA increases, the solubility of 1,1,1-TCA is relatively small resulting in relatively small effective solubility and small mass transfer rate. So it is concluded that the combination of the mole fraction and DNAPL solubility are factors in the increase in the mass depletion time.

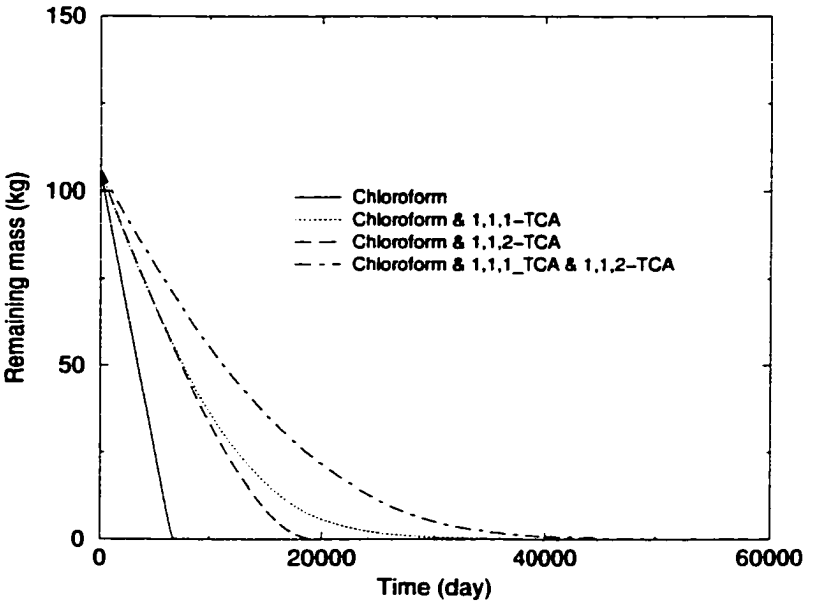

Figure 5.44: Remaining mass of Chloroform for v = 0.01 m/day

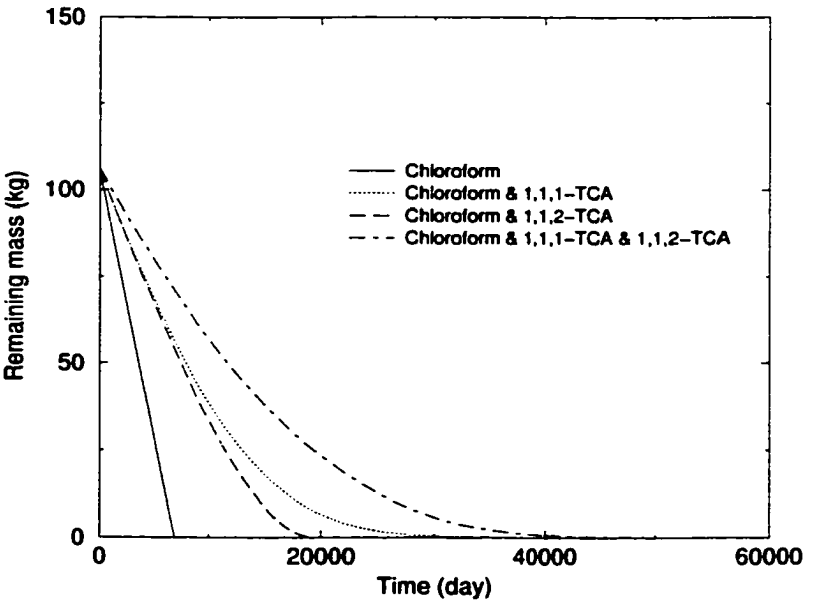

Figure 5.45: Remaining mass of Chloroform for v = 0.1 m/day

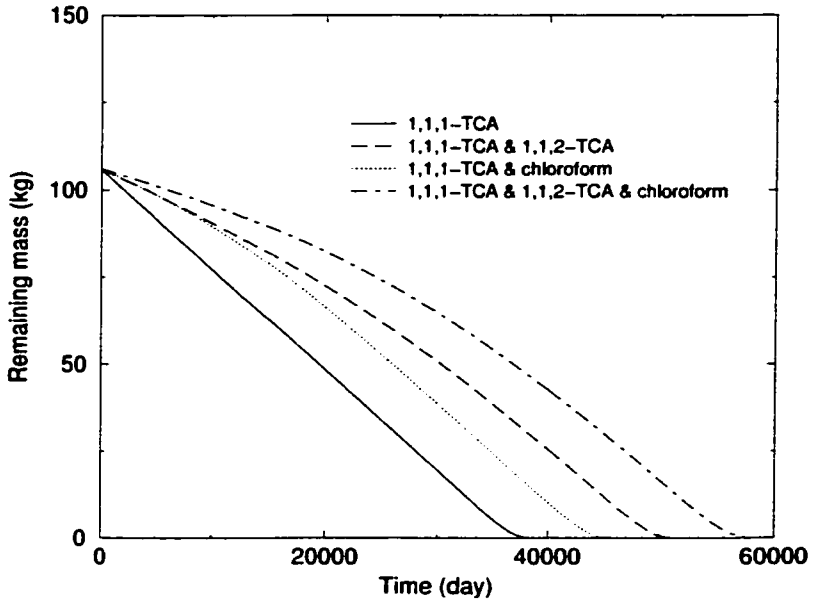

Figure 5.46: Remaining mass of 1,1,1-TCA for v = 0.01 m/day

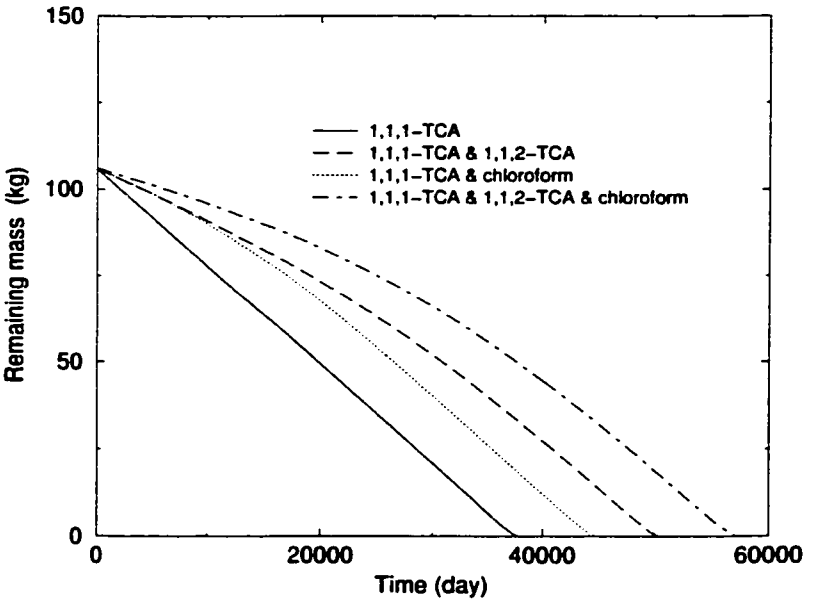

Figure 5.47: Remaining mass of 1,1,1-TCA for v = 0.1 m/day

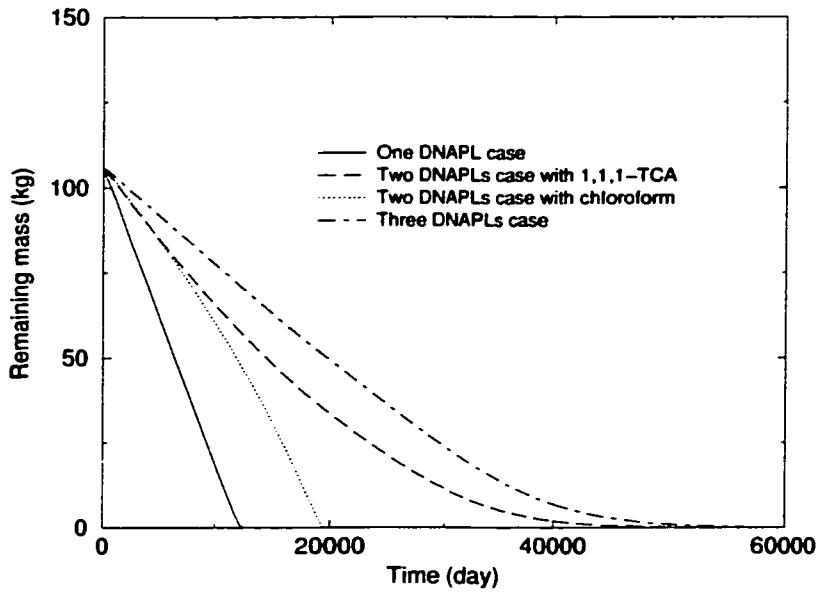

Figure 5.48: Remaining mass of 1,1,2-TCA for v = 0.01 m/day

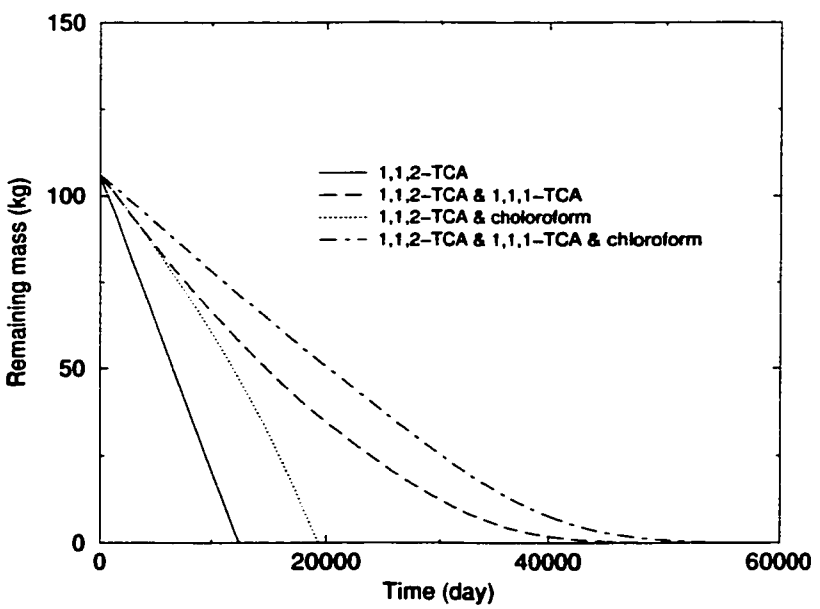

Figure 5.49: Remaining mass of 1,1,2-TCA for v = 0.1 m/day

CHAPTER 6

Conclusions

In this research, a semi-analytical method is used to examine DNAPL dissolution. A parameter called the field-scale mass transfer rate coefficient is developed. Several scenarios of DNAPL dissolution were investigated.

6.1 Summary

A DNAPL source zone consists of several subzones that contain the DNAPL. The shape of these subzones are often in form of thin, horizontal lenses or pools. Each subzone is connected by vertical fingers. In this research, the DNAPL source zone is assumed to be in a saturated, isotopic and homogeneous porous medium. The groundwater flow is uniform and steady state.

In a DNAPL-water system, interphase mass transfer occurs until equilibrium is reached. The mass transfer rate is a function of the difference in concentration between the chemical at the interface and the bulk aqueous-phase concentration and the mass transfer rate coefficient. The mass transfer rate coefficient is a lumped parameter that contains the mass transfer coefficient and the interfacial area between the NAPL and water. Mathematical solutions to the transient transport equations were used to estimate the aqueous-phase concentration in uniform groundwater flow.

Solutions were developed for a single component DNAPL in a subzone and a multi-component DNAPL in a subzone and in several subzones. Field-scale dissolution

with a multi-component DNAPL was also investigated. The solution for dissolution of a multi-component DNAPL in several subzones can be used to compute field-scale dissolution. However, in practice there is always a lack of data concerning the location and geometry for DNAPL subzones. Furthermore, calculation of several examples of multi-component DNAPL dissolution in several subzones demonstrates that the computations take a very long time. For these reasons, a new parameter called the field-scale mass transfer rate coefficient is introduced. The field-scale mass transfer rate coefficient is a lumped parameter that does not require knowledge of the location and geometry of DNAPL subzones.

Finally, several case studies were investigated. DNAPL used as examples in this research were 1,1,1-TCA, 1,1,2-TCA and chloroform. These DNAPLs exhibits a wide range of solubility and provide the opportunity to demonstrate the effect of this characteristics on the dissolution process. One, two, and three component DNAPLs were studied. The source zone was treated as one block and the field-scale mass transfer rate coefficient was used. The program written in Fortran77 provides results in terms of bulk aqueous-phase concentration, mass transfer rate, remaining DNAPL mass and mole fraction. The integrations inherent in the solution were handled by the IMSL Math/Library, the Fortran subroutines for mathematical applications.

6.2 Results and conclusions

6.2.1 The field-scale mass transfer rate coefficient

The field-scale mass transfer rate coefficient for 1,1,1-TCA, 1,1,2-TCA and chloroform were estimated at seepage velocities of 0.01 and 0.1 m·day^{-1}. The results show that the field-scale mass transfer rate coefficient is a function of the field-scale DNAPL saturation. However, the field-scale mass transfer rate coefficient for all three DNAPLs is practically constant at a sufficiently large field-scale DNAPL saturation (at the

DNAPL saturation of 0.01 for a seepage velocity of 0.01 m·day^{-1} and at DNAPL saturation of 0.001 for a seepage velocity of 0.1 m·day^{-1}.) The maximum value of the field-scale mass transfer rate coefficient of three DNAPLs are rather similar. The field-scale mass transfer rate coefficient at the velocity of 0.01 m·day^{-1} is slightly less than the field-scale mass transfer rate coefficient at the velocity of 0.1 m·day^{-1} for all three DNAPLs. This suggests that that the field-scale mass transfer rate coefficient is not strongly dependent on the seepage velocity.

6.2.2 A single component DNAPL

For a single-component DNAPL, the results show that DNAPL dissolution is slower for the less soluble DNAPL than for the more soluble one. At two velocities studied, the mass depletion time is similar for the more soluble DNAPLs (1,1,2-TCA and chloroform). The difference in the mass depletion time at the two velocities is about a year (the mass depletion time for 1,1,2-TCA is 34 and 35 years at velocities of 0.01 and 0.1 m·day^{-1}, respectively and the mass depletion time for chloroform is 19 and 20 years at velocities of 0.01 and 0.1 m·day^{-1}, respectively). On the other hand, the mass depletion time for the low solubility DNAPL(1,1,1-TCA) is much different for two velocities. The difference in the mass depletion time in this case is about 5 year (the mass depletion time for 1,1,1-TCA is 109 and 104 years at velocities of 0.01 and 0.1 m·day^{-1}, respectively). This may suggest that the seepage velocity of the groundwater has less effect on the mass transfer rate of DNAPL with relatively high solubility than of DNAPL with relatively low solubility.

Mass transfer rates for all three DNAPLs behave similarly and can be categorised into three stages. Mass transfer rates are very high at early time due to the large concentration difference between the concentration at the interface and the bulk aqueous-phase concentration which is equal to zero initially. The mass transfer rate then

decreases rapidly because the aqueous-phase concentration increases. Then, mass transfer rates are practically at steady state. The steady state mass transfer rate is resulted by the constant field-scale mass transfer rate coefficient. At the last stage, when the DNAPL mass is almost depleted then the field-scale mass transfer rate coefficient begins to decline significantly as the the DNAPL saturation decreases. The decrease in the field-scale mass transfer rate coefficient causes reduction in the mass transfer rate at later time.

The aqueous-phase concentration is initially zero since the incoming groundwater flow is assumed to be free of any contaminant. The concentration increases rapidly and reaches a nearly constant level. Once the DNAPL mass is depleted, the concentration decreases as the dissolved chemical is advected from the source zone.

6.2.3 Multi-component DNAPLs

For multi-component DNAPLs, the results show that the mass transfer rates of each component change with time. The change in the mass transfer rate is due to the change in the mole fraction of each component in the DNAPL, which changes the effective solubilities. The change in the mass transfer rate also results in a change in bulk aqueous-phase concentrations of each component with time. The concentration of the more soluble DNAPL component is relatively high at early time but decreases rapidly as time passes. The concentration of the less soluble component slowly increases until the DNAPL mass is depleted at which times all concentrations decrease due to transport from the source zone. It should be noted that concentrations of the less soluble component are still relatively high when the DNAPL mass is almost depleted. This suggests that the removal of the DNAPL mass has to be nearly completed in order to get the relatively low concentration.

The mass depletion time of each component in a multi-component DNAPLs is

about the same for both velocities studied, even though there is a great difference in the solubility in each component. This is because the effective solubility and, therefore, the mass transfer rate is now influenced by the mole fraction of each component. At early time, the more soluble component dissolves faster causing its mole fraction to decrease rapidly. At the same time, the mole fraction and effective solubility of the less soluble component increases. At late time, the more soluble component is a relatively small component of the DNAPL and, therefore the mass transfer rate of the more soluble component is small. This causes the mass depletion time to be longer despite of its high solubility. In the mean time, the less soluble component has become dominant in the DNAPL but its solubility is small resulting in small effective solubility. The mass transfer rate of the less soluble component is small also. As a result, at late time, mass transfer rates of all components in the system are small regardless of their solubility. Therefore, even with large differences in solubility, the mass of all components in the system depletes at about the same time.

A multi-component DNAPL, in groundwater with a seepage velocity of 0.01 $m \cdot day^{-1}$ takes longer to deplete than multi-component DNAPLs in groundwater with a seepage velocity of 0.1 $m \cdot day^{-1}$. Component mixtures in which both component have relatively high solubility (i.e. the mixture of 1,1,2-TCA and chloroform) takes less time to deplete than does the mixture in which both components have relatively low solubility or the mixture of components with relatively low and high solubility (i.e. mixture of 1,1,1-TCA and chloroform and mixture of 1,1,2-TCA and 1,1,1-TCA). The mass transfer rate again is strongly influenced by the mole fraction. If all components in the mixtures have high solubilities, even the component with lower solubility will have relatively high solubility, resulting in high mass transfer rates. While in the mixture with relatively high and low solubilities, the less soluble component, even at a

high mole fraction still has a relatively low effective solubility, resulting in a relatively low mass transfer rate. Therefore, mass depletion in this case takes longer.

Finally, mathematical solutions show that having more DNAPL components in the system increases the mass depletion time. In fact, the more DNAPL components there are, the longer the mass depletion time is. The combination of the mixture is also a factor in the mass depletion time.

BIBLIOGRAPHY

[1] Acree, S. D., R. R. Ross, M. R. Scalf, E. R. Graber, J. W. Mercer, and R. M. Cohen. Dense nonaqueous phase liquids-a work shop summary. Technical report, United State Environmental Protection Agency, February 1992. EPA/600/R-92/030.

[2] Afifi, S. M. F. E. D. Analytical solutions for contaminant groundwater transport. Master's thesis, Colorado State University, 1990.

[3] Banerjee, S. Solubility of organic mixtures in water. *Environmental Science and Technology*, 18:587–591, 1984.

[4] Broholm, K. and S. Feenstra. Laboratory measurements of the aqueous solubility of mixtures of chlorinated solvents. *Environmental Toxicology and Chemistry*, 14(1):9–15, 1995.

[5] Cherry,J. A., S. Feenstra, and D.M. Mackay. Developing a conceptual framework and rational goals for groundwater remediation at dense nonaqueous phase liquid sites. *Third Intern. Conf. on Ground Water Quality Research, Dallas, TX*, June 21 –24 1992.

[6] Chrysikopoulos, C. V. Three-dimensional analytical models of contaminant transport from nonaqeous phase liquid pool dissolution in saturated subsurface formation. *Water Resources Research*, 31(4):1137–1145, 1995.

[7] Chrysikopoulos, C. V. and K. Y. Lee. Contaminant transport resulting from multicomponent non-aqueous phase liquid pool dissolution in three-dimensional subsurface formations. *Journal of Contaminant Hydrology*, 31:1–21, 1998.

[8] Corey, A. T. *Mechanics of immiscible fluids in porous media.* Water Resources Publications, 1986. Littleton, Colorado.

[9] Feentra, S. *Aqueous concentration ratios to estimate mass of multi-component NAPL residual in porous media.* PhD thesis, University of Waterloo, 1997.

[10] Freeze, R. A. and D. B. McWhorter. A framework for assessing risk reduction due to dense nonaqueous phase liquid mass removal from low-permeability soils. *Ground Water*, 35(1):111–123, 1997.

[11] Geller, J. T. and J. R. Hunt. Mass transfer from nonaqueous phase organic liquids in water-saturated porous media. *Water Resources Research*, 29(4):833–845, 1993.

[12] Grubb, D. G. and N. Sitar. Evaluation of technologies for in-situ cleanup of DNAPL contaminated sites. Technical report, United State Environmental Protection Agency, September 1994. EPA/600/SR-94/120.

[13] Hunt, B. Dispersive sources in uniform groundwater flow. *The American Society of Civil Engineerings - Journal of the Hydraulics Division*, 104:75–85, 1978.

[14] Hunt, J. R., N. Sitar, and K. S. Udell. Nonaqueous phase liquids transport and cleanup. 1. analysis of mechanisms. *Water Resources Research*, 24(8):1247–1258, August 1988.

[15] Imhoff, P. T., P. R. Jaffe, and G. F. Pinder. An experimental study of complete dissolution of a nonaqueous phase liquid in saturated porous media. *Water Resources Reseach*, 30(2):307–320, 1993.

[16] Kim, T. and C. V. Chrysikopoulos. Mass transfer correlations for nonaqueous phase liquid pool dissolution in saturated porous media. *Water Resources Research*, 35(2):449–459, February 1999.

[17] Kueper, B. H., W. Abbot, and G. Farguhar. Experimental observations of multiphase flow in heterogeneous porous media. *Journal of Contaminant Hydrology*, 5:83–95, 1989.

[18] Mackey, D., W. Y. Shiu, A. Maijanen, and S. Feenstra. Dissolution of nonaqueous phase liquids in groundwater. *Journal of Contaminant Hydrology*, 8:23–42, 1991.

[19] Mayer, A. S. and C. T. Miller. The influence of mass transfer characteristics and porous media heterogeneity on nonaqueous phase dissolution. *Water Resources Research*, 32(6):1551–1567, 1996.

[20] Miller, C. T., M. M. Poirier-McNeill, and A. S. Mayer. Dissolution of trapped nonaqueous phase liquids; mass transfer characteristics. *Water Resources Research*, 26(11):2783–2796, November 1990.

[21] Montgomery, J. H. *Groundwater chemicals desk reference.* Lewis publishers, Boca Raton, Fla, 1996. 2nd edition.

[22] Pankow, J. F. and J. A. Cherry. *Dense chlorinated solvent and other dense non-aqueous phase liquids in groundwater: history, behavior, and remediation.* Waterloo press, Ontario, Canada, 1996.

[23] Powers, S. E., L. M. Abriola, and W. J. Weber Jr. An experimental investigation of nonaqueous phase liquid dissolution in saturated subsurface systems: Steady state mass transfer rates. *Water Resources Research*, 28(10):2691–2705, 1992.

[24] Powers, S. E., L. M. Abriola, and W. J. Weber Jr. An experimental investigation of nonaqueous phase liquid dissolution in saturated subsurface systems: Transient mass transfer rates. *Water Resources Research*, 30(2):321–332, 1994.

[25] Powers, S. E., C. O.Loureiro, L. M. Abriola, and W. J.Weber Jr. Theoretical study of the significance of nonequilibrium dissolution of nonaqueous phase liquids in subsurface systems. *Water Resources Research*, 27(4):463–477, 1991.

[26] Saba, T. and T. H. Illangasekare. Effect of groundwater flow dimensionality on mass transfer from entrapped nonaqueous phase liquid contaminants. *Water Resources Research*, 36(4):971–979, 2000.

[27] Sale, T. C. and D. W. McWhorter. Steady state mass transfer from single-component dense non-aqueous phase liquids in uniform flow fields. *Water Resources Research*, 37(2):393–404, February 2001.

[28] Schwille, F. *Dense Chlorinated Solvents in Porous and Fractured Media: Model Experiments.* Lewis Publishers, 1988. translated from the German by J. F. Pankow.

[29] Sherwood, T. K., R. L. Pigford, and C. R. Wilke. *Mass Transfer.* McGraw-Hill, 1975.

[30] Shiu, W. Y., A. Maijanen, A. L. Y. Ng, and D. Mackay. Preparation of aqueous solutions of sparingly soluble organic substances, ii. multicomponent systems -

hydrocarbon mixtures and petroleum products. *Environmental Toxicology and Chemistry*, 7:125–137, 1988.

[31] Van Genuchten, M. T. and W. J. Alves. Analytical solutions of the one-dimensional convective-dispersive solute transport equation. Technical report, U.S. Department of Agriculture, Washington,D.C., 1982.

[32] Whelan, M. P., E.A. Voudrias, and A. Pearce. DNAPL pool dissolution in saturated porous media: procedure development and preliminary results. *Journal of Contaminant Hydrology*, 15:223–237, 1994.

[33] Zhu, J. and J. F. Sykes. The influence of NAPL dissolution characteristics of field-scale contaminant transport in subsurface. *Journal of Contaminant Hydrology*, 41:133–154, 2000.

APPENDIX A

Continuous mass release in a prism

The solution for an instantaneous point release is;

$$C = \frac{M_o}{\phi} f_1(x_1,t) f_2(x_2,t) f_3(x_3,t) \tag{A.1}$$

where M_o is mass release, ϕ is porosity and

$$\begin{aligned} f_1(x_1,t) &= \frac{1}{2\sqrt{\pi D_{11} t/R}} \exp\left[\frac{-(x_1 - v_1 t/R)^2}{4D_{11} t/R}) - \mu t\right] \\ f_2(x_2,t) &= \frac{1}{2\sqrt{\pi D_{22} t/R}} \exp(\frac{-x_2^2}{4D_{22} t/R}) \\ f_3(x_3,t) &= \frac{1}{2\sqrt{\pi D_{33} t/R}} \exp(\frac{-x_3^2}{4D_{33} t/R}) \end{aligned}$$

Eqn. (A.1) is for the case where the point of release is located at $x_1 = x_2 = x_3 = 0$. When the point of release is located at any arbitary, supposedly at $(\hat{x}_1, \hat{x}_2, \hat{x}_3)$, then the solution will be;

$$C = \frac{M_o}{\phi} f_1(x_1 - \hat{x}_1, t) f_2(x_2 - \hat{x}_2, t) f_3(x_3 - \hat{x}_3, t) \tag{A.2}$$

If point sources are to line up continuously along x_2 with a finite length from $-L_2$ to L_2 as shown in figure (A.1), the line source will be created. Suppose M_1 is the uniform quantity of mass released per unit length of line. An instantaneous point release at $(\hat{x}_1, \hat{x}_2, \hat{x}_3)$ is approximated by;

$$M_o = M_1 2L_2 \tag{A.3}$$

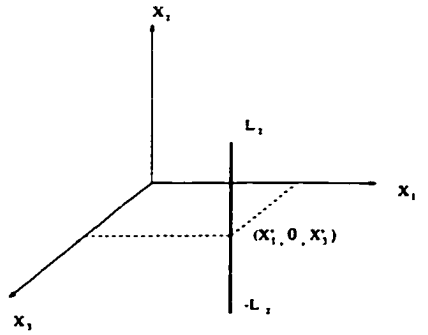

Figure A.1: Instantaneous line source

Substitute M_o into eqn. (A.1), and integrate the point source solution from $-L_3$ to L_3. The concentration resulted from a line source parallel to x_3 and located at $\hat{x}_1 = \hat{x}_3 = 0$ can be obtained;

$$C = \frac{M_1}{\phi} \int_{-L_2}^{L_2} f_1(x_1 - \hat{x}_1, t) f_2(x_2 - \hat{x}_2, t) f_3(x_3 - \hat{x}_3, t) dx_2 \quad \text{(A.4)}$$

$$= \frac{M_1}{\phi} f_1(x_1 - \hat{x}_1, t) F_2(x_2 - \hat{x}_2, t) f_3(x_3 - \hat{x}_3, t) \quad \text{(A.5)}$$

where

$$F_2(x_2 - \hat{x}_2, t) = \int_{-L_2}^{L_2} f_2(x_2 - \hat{x}_2, t) d\hat{x}_2$$

$$= \frac{1}{2} \left[\text{erf}\left(\frac{x_2 + L_2}{2\sqrt{D_{22} t/R}}\right) - \text{erf}\left(\frac{x_2 - L_2}{2\sqrt{D_{22} t/R}}\right) \right]$$

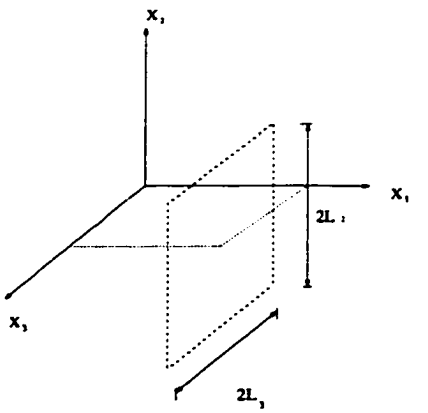

Figure A.2: Instantaneous plane source

In the same procedure, in order to get the solution for instantaneous mass release from a plane, an instantaneous point release solution is integrated over the finite plane. Suppose a plane source lines parallel with x_2 and x_3 plane and has dimension of $2L_2 * 2L_3$ as shown in figure (A.2). Then, the solution for mass release in plane is;

$$C = \frac{M_2}{\phi}\int_{-L_2}^{L_2}\int_{-L_3}^{L_3} f_1(x_1-\hat{x}_1,t)f_2(x_2-\hat{x}_2,t)f_3(x_3-\hat{x}_3,t)dx_2dx_3 \quad \text{(A.6)}$$

$$= \frac{M_2}{\phi} f_1(x_1-\hat{x}_1,t)F_2(x_2-\hat{x}_2,t)F_3(x_3-\hat{x}_3,t) \quad \text{(A.7)}$$

where M_2 is mass per unit area and

$$F_3(x_3-\hat{x}_3,t) = \int_{-L_3}^{L_3} f_3(x_3-\hat{x}_3,t)dx_3$$

$$= \frac{1}{2}\left[\text{erf}(\frac{x_3+L_3}{2\sqrt{D_{33}t/R}}) - \text{erf}(\frac{x_3-L_3}{2\sqrt{D_{33}t/R}})\right]$$

And lastly, the solution for instantaneous mass release in prism is;

$$C = \frac{M_3}{\phi} F_1(x_1-\hat{x}_1,t)F_2(x_2-\hat{x}_2,t)F_3(x_3-\hat{x}_3,t) \quad \text{(A.8)}$$

where M_3 is mass per unit volume and

$$F_1(x_1-\hat{x}_1,t) = \int_{-L_1}^{L_1} f_1(x_1-\hat{x}_1,t)dx_1$$

$$= \frac{e^{-\mu t}}{2}\left[\text{erf}(\frac{x_1+L_1-v_1t/R}{2\sqrt{D_{11}t/R}}) - \text{erf}(\frac{x_1-L_1-v_1t/R}{2\sqrt{D_1t/R}})\right]$$

In this study mass is considered to be released from any DNAPL subzone. Thus, mass input in mathematical model has to be a continuously released mass. First, consider an instantaneous point release at $x_1 = x_2 = x_3 = 0$ which to be released at $time = 0$. The concentration at any position and any time can be calculated from eqn.(A.1). Suppose instantaneous point mass is released at $time = \tau$, then the concentration can be calculated as;

$$C = \frac{M_o}{\phi} f_1(x_1,t-\tau)f_2(x_2,t-\tau)f_3(x_3,t-\tau) \quad \text{(A.9)}$$

Because the differential equation is linear, the response of each instantaneous point mass can be superimposed at different time. Let M_{o1} is instantaneous point mass released at $time = \tau_1$ and gives the concentration of $C(\tau_1)$ and M_{o2} is instantaneous point mass released at $time = \tau_2$ and gives the concentration of $C(\tau_2)$; then the concentration at any time greater than τ_2 is;

$$C(t) = C(\tau_1) + C(\tau_2) \qquad where\ t \geq \tau_2 \geq \tau_1 \tag{A.10}$$

From this idea, suppose a sequence of instantaneous point mass are continously released over a very small interval of time, $\triangle\tau$ for the total of time τ. So total mass released over time τ can be written as;

$$M_o = \frac{\triangle M_o}{\triangle \tau}\tau \tag{A.11}$$

where $\frac{\triangle M_o}{\triangle \tau}$ is the rate of mass release and $\sum_{i=1}^{n} \triangle\tau_i = \tau$. Suppose there are n instantaneous point mass released in n time intervals. Therefore, the concentration for instantaneous point mass release over time τ is;

$$C = \frac{1}{\phi}\sum_{i=1}^{n} \frac{\triangle M_o}{\triangle \tau}|_{\tau_i} f_1(x_1, t-\tau_i) f_2(x_2, t-\tau_i) f_3(x_3, t-\tau_i)\triangle\tau_i \tag{A.12}$$

Suppose $\triangle\tau$ is so small until $\triangle\tau \rightarrow 0$ then;

$$C = \frac{1}{\phi}\int_0^t \frac{dM_o}{d\tau} f_1(x_1, t-\tau) f_2(x_2, t-\tau) f_3(x_3, t-\tau) d\tau \tag{A.13}$$

Then the solution for continuous mass release in prism is;

$$C = \frac{1}{\phi}\int_0^t \dot{M}_o F_1(x_1, t-\tau) F_2(x_2, t-\tau) F_3(x_3, t-\tau) d\tau \tag{A.14}$$